PhD Program of Clinical and Experimental Medicine (CEM)

XXXV Doctorate Cycle

Director of the PhD Program: Prof. Marco Vinceti

Bone and metallic augmented reverse shoulder arthroplasty to preserve glenoid bone in shoulder osteoarthritis: analysis of radiographic features and patient outcomes

Supervisor

Giuseppe Porcellini

Candidate

Giovanni Merolla

INDEX

ABSTRACT (IT)

Introduzione: La protesi inversa rappresenta una opzione valida per il trattamento dell'artrosi di spalla con severa deformità ossea glenoidea, ma richiede un alesaggio correttivo esteso per il ripristino della versione ed inclinazione glenoidea nativa, con relativi rischi di medializzazione della glenoide e fallimento della fissazione. L'utilizzo di un innesto osseo, prelevato dalla testa omerale e fissato sul "baseplate" all' interfaccia della glenoide nativa, è stato proposto per minimizzare l'alesaggio glenoideo e ripristinare il bone stock glenoideo ("Bony-Increased Offset, BIO- RSA"). Il "baseplate" aumentato metallico ("Metallic-Increased Offset – MIO-RSA"), rappresenta un'alternativa alla BIO-RSA per ripristinare la interlinea articolare. Ad oggi, persistono ancora delle controversie sulla scelta del "bone graft" o dell' "augment" metallico nella protesi inversa di spalla lateralizzata.

Obiettivi: Abbiamo testato due ipotesi: i) la MIO-RSA previene la medializzazione della linea articolare e garantisce risultati clinici e un tasso di "scapular notching" simile alla BIO-RSA; ii)la integrazione del graft osseo nella BIO-RSA è compromessa nel tempo, aumentando il rischio fallimento della fissazione a lungo termine.

Materiali e Metodi: Abbiamo arruolato in modo retrospettivo 81 pazienti (83 spalle) sottoposti a BIO-RSA (44) o MIO-RSA (39). La deformità glenoidea primaria (A1, A2, B1, B2, B3, C, D) e secondaria a rottura di cuffia (E1, E2, E3, E4), è stata classificata secondo specifici criteri, utilizzando la tomografia computerizzata. La mobilità attiva e il "Western Ontario Osteoarthritis of the Shoulder (WOOS) Index" sono stati usati per la misura dell' "outcome" clinico.

Tutte le alterazioni radiografiche postoperatorie dell'impianto sono state valutate all'ultimo follow-up. Presenza e dimensione delle linee di radiolucenza glenoidea sono state utilizzate per valutare la integrazione del "bone graft" (gruppo BIO-RSA) e il "baseplate seating" (gruppo MIO-RSA) (assenza di radiolucenza: "perfect seating"; linee di radiolucenza < 2 mm: "incomplete seating"; linee di

radiolucenza > 2 mm: mobilizzazione). Abbiamo valutato lo spessore del "bone graft" (mm), la posizione della glenosfera sulla glenoide (alta, centrata, bassa, molto bassa), la versione (metodo di Friedman) e la inclinazione (angolo "**β**") glenoidea preoperatoria e postoperatoria.

Risultati: Al follow-up medio di 36.5 mesi gli "scores" preoperatori e postoperatori sono aumentati in modo significativo in entrambi i gruppi ($p < 0.001$). Il punteggio delta della elevazione anteriore attiva è risultato più alto nel gruppo MIO-RSA ($p = 0.027$). Non sono state riscontrate differenze significative negli altri piani di movimento e nei punteggi del WOOS index tra i due gruppi. La retroversione glenoidea preoperatoria è stata maggiore nei pazienti del gruppo BIO-RSA, mentre la inclinazione glenoidea è stata simile nei due gruppi. Le glenoidi di tipo B2 e B3 avevano una erosione postero-centrale (91%) e postero-superiore (90%) con una rispettiva sublussazione posteriore della testa omerale in media del 76% e 78%. La direzione della erosione riscontrata nelle glenoidi tipo E2 e E3 è stata di tipo postero-superiore, con una media di sublussazione posteriore della testa omerale del 74%.

Il tasso di posizione alta della glenosfera è stato maggiore nel gruppo BIO-RSA ($p = 0.022$),

Il gruppo BIO-RSA ha mostrato linee di radiolucenza intorno al graft osseo in 16 pazienti (36.4%) e riduzione dello spessore in 15 (34.1%). Un "seating" incompleto del baseplate è stato riscontrato in 3 pazienti del gruppo MIO-RSA (7%). Abbiamo trovato un più alto tasso di linee di condensazione omerale nel gruppo MIO-RSA e un più alto tasso di assottigliamento corticale ($p=0.01$) e riassorbimento tuberositario nel gruppo BIO-RSA (rispettivamente, $p= 0.027$ e $p = 0.004$).

Conclusioni: I risultati clinici simili, ottenuti con i modelli BIO-RSA e MIO-RSA, confermano la prima ipotesi dello studio. Il "baseplate seating" completo riscontrato in > 90% dei pazienti con MIO-RSA esprime la eccellente stabilità e capacità di fissazione del metallo. Il tasso di riassorbimento del "bone graft" conferma la seconda ipotesi dello studio sui potenziali rischi di fallimento del "baseplate" a lungo termine.

Parole chiave: *spalla, artroplastica inversa, glenoide, graft osseo, baseplate aumentato*

ABSTRACT (EN)

Background : Reverse shoulder arthroplasty (RSA) is a valid option to address shoulder osteoarthritis with severe glenoid deformity, but requires an extensive reaming to restore the native version with high risk of baseplate failure. The use of autologous bone graft harvested from the humeral head and fixed on the baseplate at the interface of the native glenoid, was proposed to minimize glenoid reaming and restore glenoid bone stock (Bony-Increased Offset, BIO- RSA).

Metallic-augmented glenoid components (Metallic-Increased Offset – MIO-RSA) have been proposed as viable alternative to BIO-RSA, preserving more native bone stock and restoring the joint line, with a final goal of increasing the baseplate support.

Thus, controversies still exist about the choice of bone grafting or metal augments in RSA.

Objectives: In this study we tested two hypotheses: i) metal augmented baseplate give similar clinical outcomes and rate of scapular notching, and prevents the medialization of the joint line similarly to BIO-RSA; ii) bone graft viability and healing in BIO-RSA patients are impaired over time, thus making concern about baseplate fixation and stability in the long-term.

Materials and methods: Eighty-one patients (83 shoulders) underwent glenoid lateralization with bone (BIO-RSA group, 44) or metal augmented baseplate (MIO-RSA group, 39). The orientation and direction of glenoid erosion was identified and recorded using computerized 3D planning. Active range of motion, and the Western Ontario Osteoarthritis of the Shoulder (WOOS) index were assessed before arthroplasty and at the last follow-up visits.

Radiographic changes around the glenoid and humeral components were assessed. Healing and thickness of bone graft were evaluated by predefined criteria. Postoperative global glenoid inclination (**β** angle) and retroversion were also measured.

Results: At a mean of 36.5 months preoperative and postoperative clinical scores improved significantly in both groups ($p < 0.01$). Delta scores of active anterior elevation were higher in the MIO-RSA group ($p = 0.027$). The differences in the other planes of shoulder motion and in WOOS index scores between the groups were not significant. Preoperative glenoid retroversion was higher in BIO-RSA patients, glenoid inclination was similar in both groups.

Type B2 and B3 glenoids had a posterior-central (91%) and posterior-superior (90%) erosion with a mean posterior humeral head subluxation of 76% and 78%, respectively. The direction of erosion in Type E2 and E3 glenoids was posterior-superior, with a mean posterior humeral head subluxation of 74%.

The rate of high position of the glenosphere was higher in the BIO-RSA group ($p = 0.022$), while the values of **β** angle and postoperative retroversion were similar in the two groups. BIO-RSA group showed radiolucent lines < 2mm around the bone graft in 16 patients (36.4%) and decreased thickness in 15 (34.1%). Incomplete baseplate seating was found in 3 MIO-RSA patients (7%).

We found higher rate of humerus condensation lines in MIO-RSA patients ($p = 0.01$) and higher rate of cortical thinning and tuberosity resorption in the BIO-RSA group ($p = 0.027$ and $p = 0.004$, respectively).

Conclusion: Metal augmented glenoid is a suitable alternative to BIO-RSA to preserve bone and prevent the medialization of the joint line in arthritic glenoid with multiplanar glenoid deformity. Bone and metal augmentation provided both satisfactory clinical outcomes. Bone graft resorption in BIO-RSA patient raise concern about the risk of baseplate loosening and requires further long term studies.

Key words: *shoulder, reverse arthroplasty, glenoid, bone grafting, augmented baseplate*

CHAPTER 1

Introduction

1.1 Clinical anatomy of the shoulder

1.1.1 **The shoulder complex**

The shoulder is a joint responsible for articulation of the upper extremities with the trunk or axial skeleton. It plays a key role in the function of the arms and hands, the dexterity of which sets human beings apart from many other mammals. With the demands of strength, endurance, and flexibility that are placed on the shoulder through everyday life, it often becomes a source of musculoskeletal complaints and pathology. Therefore, it is a structure that health care providers should be comfortable evaluating.

1.1.2 **Skeletal**

The shoulder complex comprises several bony structures that play an important role in normal shoulder function[1]. The clavicle is the only bony attachment that connects the glenohumeral joint to the axial skeleton. Its articulation with the sternum and acromion process allows the clavicle to function as a strut, suspending the glenohumeral joint from the axial skeleton[2,3]. The broad, flat acromion is the most lateral part of the scapula and articulates with the clavicle through the diarthrodial acromiolavicular joint and also serve as attachment site for several muscles and ligaments. The coracoid process is an excellent landmark for many shoulder procedures. It lies medial and anterior to the glenohumeral joint and is the attachment site for the conjoined tendon of the coracobrachialis muscle and short head of the biceps muscles. The coracoacromial ligament connects the coracoid and anterolateral acromion, thereby forming the coracoacromial arch[4]. The proximal humerus consists of the head, the surgical and anatomic neck, and the greater (lateral) and lesser (anteromedial) tuberosities. The tuberosities form an attachment sites for the rotator cuff muscles, and the bicipital groove lies between them. The glenohumeral articulation is a ball-and-socket joint formed by the shallow glenoid and the large

humeral head[5] (Figure 1 A-B and Figure 2). This lack of bony containment is unique to the glenohumeral joint and provides a wide range of motion; however, it also makes the joint prone to instability. The surrounding ligaments and muscles substantially contribute to gleno-humeral stability.

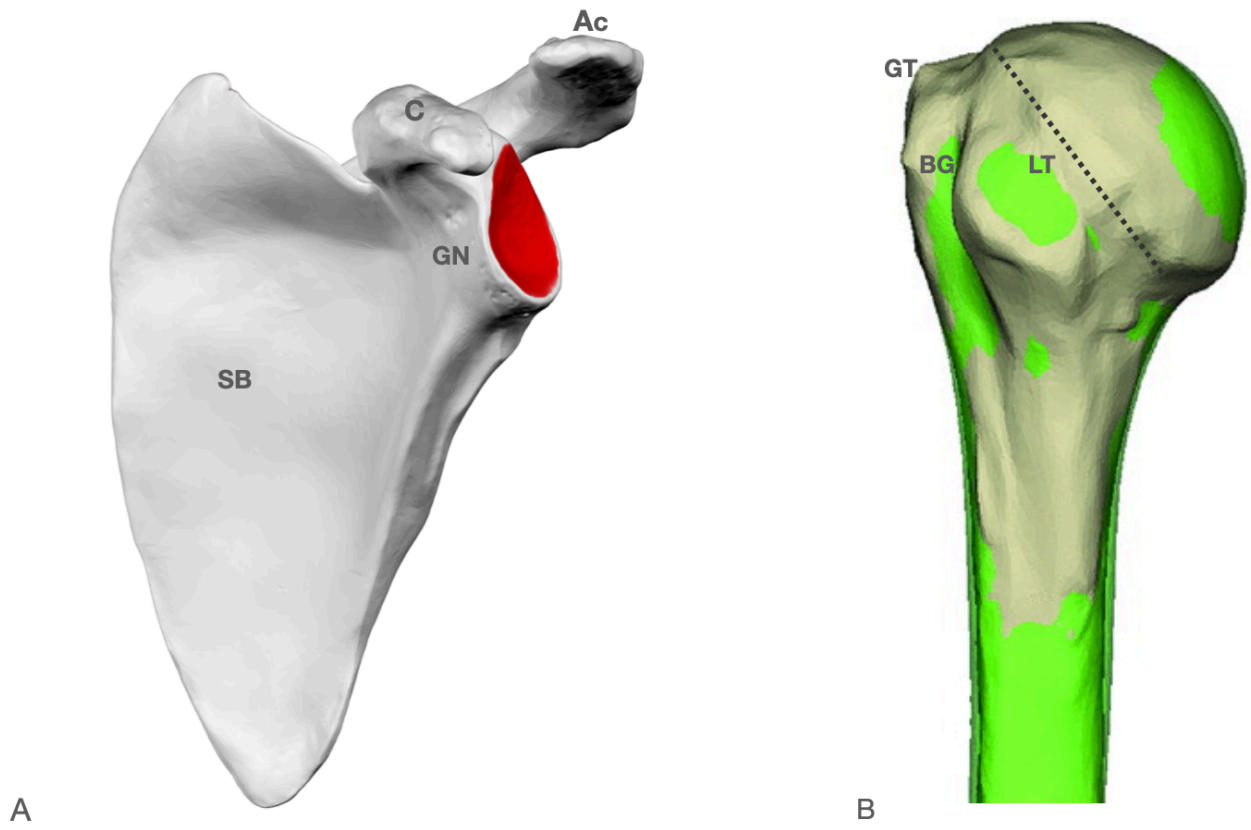

Figure 1. A, scapula and B, proximal humerus. Ac: acromion, C: coracoid, GN: glenoid neck, SB: scapular body, GT: greater tuberosity, BG: bicipiteal groove, LT: lesser tuberosity. The dotted line represents the anatomical neck and the red surface the glenoid cavity.

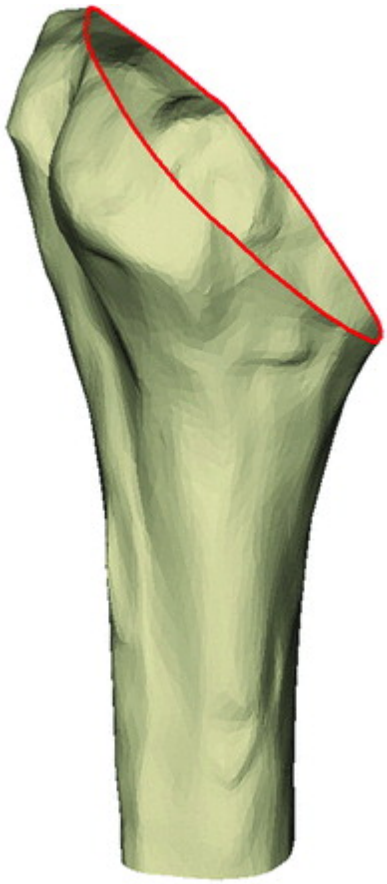

Figure 2. Humeral cut along the surgical neck.

1.1.3 **Soft tissue structures and ligaments**

The labrum surrounds the glenoid and functions to deepen the glenohumeral socket and provides an attachment site for the glenohumeral ligaments[6]. The superior glenohumeral ligament originates at the superior glenoid tubercle and blends with the anterior rotator cuff musculature and coracohumeral ligament to form the biceps pulley near the bicipital groove[7,8]. The middle glenohumeral ligament runs from the anterior labrum to the lesser tuberosity, and the inferior glenohumeral ligament connects the inferior glenoid to the inferior humerus[8-10] (Figure 3). Each glenohumeral ligament is believed to contribute to glenohumeral stability in various position of glenohumeral motion[8].

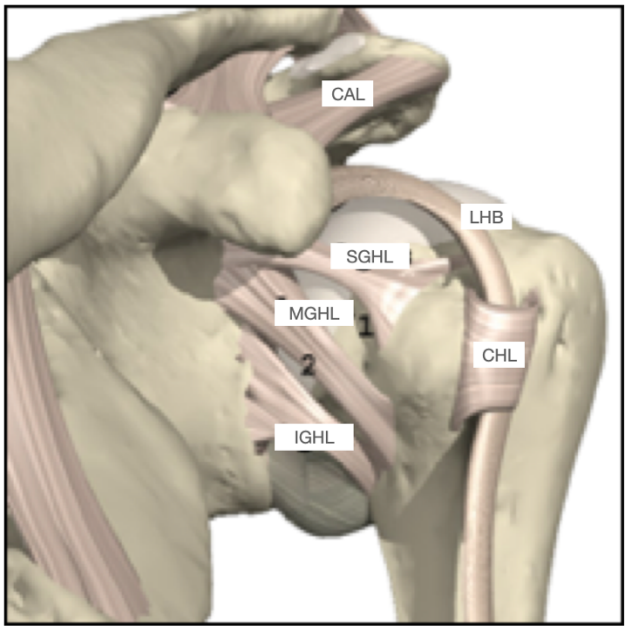

Figure 3: Main ligaments of the gleno-humeral joint and long head of the biceps (LHB). CAL: coraco-acromial ligament; SGHL: superior gleno-humeral ligament; MGHL: middle gleno-humeral ligament; IGHL: inferior gleno-humeral ligament.

1.1.4 **Shoulder muscles**

Glenohumeral motion and function are directly linked to the surrounding musculature. The deltoid consists of anterior, lateral and posterior components separated by fibrous raphes. Its proximal attachment is to the lateral third of the clavicle anteriorly, the lateral acromion, and the scapular spine posteriorly[8]. The deltoid muscle is innervated by branches of the axillary nerve and inserts at the deltoid tuberosity of the lateral humerus. Its primary function is abduction, flexion and extension of the shoulder. The coracobrachialis muscle and the pectoralis major lie medial to the deltoid. The two heads of the pectoralis major originate from the clavicle and sternum and insert lateral to the bicipital groove of the humerus[11-14]. The pectoralis major is innervated by the medial and lateral pectoral nerves and functions primarily as a humeral adductor. The coracobrachialis and the short head of the biceps lies deep to the pectoralis major and deltoid[11]. They originate from the coracoid process and are innervated by the musculocutaneous nerve. The coracobrachialis and the short head of the biceps serve as an important landmark for shoulder surgery because the brachial plexus and vascular structures lie just medial and deep to them. Th rotator cuff musculature exists deep to the deltoid muscle and surrounds the glenohumerla joint[15]. It is composed of four muscles that play an important role in glenohumeral motion and dynamic shoulder stability[15-17] (Figure 4 A-C). The subscapularis originates from the undersurface of the scapula and inserts at the lesser tuberosity. It is innervated by the upper and lower subscapular nerves and functions to internally rotate the humerus[16]. In collaboration with the infraspinatus, ths subscapularis inferiorly depresses the humerus, thereby preventing acromial impingement when the deltoid is activated[16]. The infraspinatus and teres minor originate from the posterior scapula and insert at the greater tuberosity[15-17]. They primarily function by providing an external rotation moment at different degrees of glenohumeral abduction and are innervated by the suprascapular and axillary nerve, respectively. The supraspinatus is also innervated by the supracapular

nerve and inserts at the greater humeral tuberosity[15-17]. It is responsible for initiating glenohumeral abduction, which allows the deltoid to function more efficiently[1].

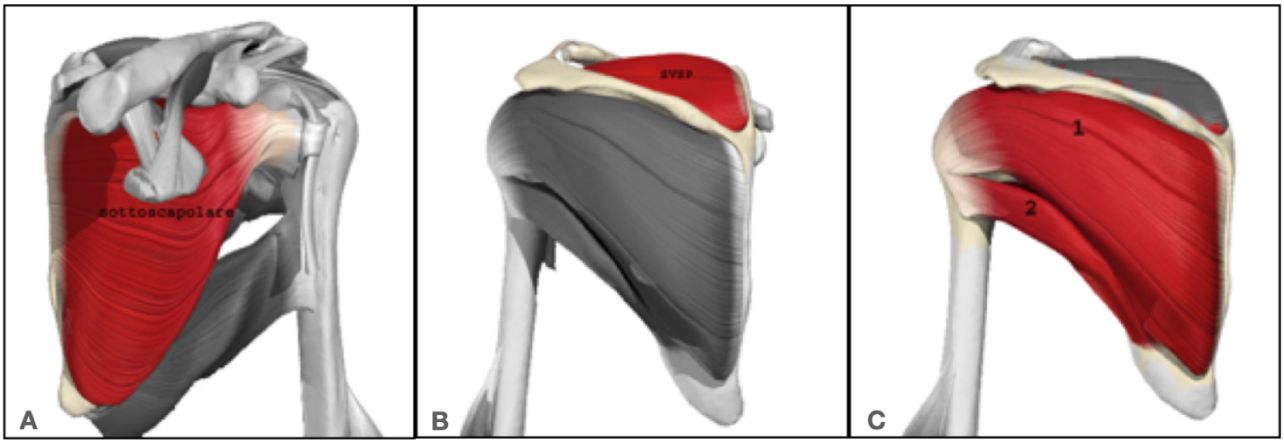

Figure 4. Rotator cuff muscles of the shoulder. A, subscapularis; B, supraspinatus; C, infraspinatus (1) and teres minor (2).

1.1.5 **Neural and vascular structures**

The axillary nerve innervates the deltoid and teres minor muscles. It originates from the posterior cord of the brachial plexus and runs along the anterior aspect of the subscapularis muscle before passing under the inferior border of the subscapularis medial to the coracoid process. The axillary nerve form two major branches as it passes under the inferior glenohumeral capsule and exits through the quadrangular space. One branch innervates the teres minor and posterior deltoid, and the other branch winds around the proximal humerus to innervates the lateral and anterior deltoid. In this lateral position, the average distance from the acromion to the axillary nerve is approximately 5 to 7 cm[18-20]. The musculocutaneous nerve originates from the lateral cord of the brachial plexus and enters the muscle belly of the coracobrachialis an average of 4 to 8 cm distal to the tip of the coracoid process[21]. From this location the nerve exits the coracobrachialis and traverses the interval between the biceps and brachialis muscles. Although the musculocutaneous nerve is not frequently encountered during surgical approaches to the glenohumeral joint, it can be injured by indiscriminate retraction of the conjoined tendon. The suprascapular nerve originates from the upper trunk of the brachial plexus and passes beneath the trapezius muscle before it passes through the suprascapular notch along the superior edge of the scapula[22]. It is likely most vulnerable to injury along the superior margin of the glenoid before entering the infraspinatus fossa[1].

The blood supply of the shoulder girdle is derived primarily from branches of the subclavian and axillary arteries[23]. The suprascapular artery accompanies the suprascapular nerve and vein over the superior edge of the scapula. In contrast to the suprascapular nerve, the suprascapular artery passes over the transverse scapular ligament and must be protected during suprascapular nerve release. The thoraco-acromial branch of the axillary artery follows the course of the coracoacromial ligament and can be injured near this location. The anterior and posterior circumflex humeral arteries encircle the humerus deep to the deltoid. The posterior circumflex artery accompanies the axillary nerve and

posterior circumflex vein, whereas the anterior circumflex artery arises deep to the coracobrachialis and runs along the inferior border of the subscapularis[23]. This vessel is frequently encountered with a delto-pectoral approach and is ligated before subscapularis mobilization.

1.1.6 **Concept of surgical anatomic layers**

Surgical anatomy of the shoulder has been described as consisting of four Layers[24]. Layer 1 consists of the deltoid and pectoralis major muscle bellies. Layer 2 is formed by the clavipectoral fascia, the conjoined tendon, and the coracoacromial ligament anteriorly and is posteriorly continuous with the clavipectoral fascia, with the posterior scapular fascia overlying the infraspinatus and teres minor muscles. The third layer is composed of the deep layer of the subdeltoid bursa and underlying rotator cuff, Layer 4 is formed by the capsule of the glenohumeral joint.

1.2 **Epidemiology, pathomechanics and classification of shoulder osteoarthritis**

Degenerative changes of the glenohumeral joint are found in up to 17% of patients with shoulder pain, a patient group that has tripled in the last 40 years[25,26]. Although symptomatic glenohumeral osteoarthritis (GHOA) is not as common as osteoarthritis of the hip and knee joints, it can be just as debilitating due to the functional importance of the upper limbs.

A recent Korean study using the Kellgren-Lawrence classification identified GHOA (K-L $\geq$ 2) in 5.2% of the population age 65 and above[27]. Two imaging studies using the Samilson-Prieto classification showed GHOA prevalence rates in the middle-aged and elderly (age above 40 and 65 years respectively) to be as high as 17%–19%, while bilateral disease was identified in 3.1%–7.7% of the population[28 29]. Prevalence rates of GHOA due to a specific identifiable cause (secondary OA) was reported at only 1.3%–1.7%, making age-related non-specific GHOA 10 times more common[28 29] (primary osteoarthritis). However, GHOA, due to a specific identifiable cause, has been shown to be significantly more common in patients age less than 50[30]. GHOA is diagnosable when anatomical changes of joint damage are identifiable as radiological features and when clinical symptoms led by joint pain occur in a patient. The pathogenesis of GHOA is a complex and still incompletely understood process with various factors affecting joint damage and joint pain. A commonly held view is that joint damage is caused by either abnormal mechanical stress on normal cartilage or normal stress on structurally weakened cartilage. These opposites represent the ends of a spectrum, with patient factors influencing the proportional effect of mechanical stress and cartilage health on the patient's risk of developing OA. Joint damage irrespective of cause, leads to a common biochemical cascade resulting in ongoing joint wear and synovitis. In the glenohumeral joint, focal or global cartilage loss and subsequent subchondral bony sclerosis are most pronounced in the upper two-thirds of the humeral head. This area is in contact with the glenoid between 60 and 100 degrees of abduction[31]. The most frequent bony change in GHOA is the formation of osteophytes, due to chondrocyte stimulation and

enchondral ossification in the transition area of the hyaline cartilage and synovial membrane. Osteophytes are predominant in the anterior-inferior aspects of the humeral head and inferior aspects of the glenoid and are thought to result from mechanical capsular traction[32] (Figure 5). Humeral osteophytes are often accompanied by enthesopathic changes at ligament attachment sites, typically involving the anatomical neck and tuberosities as well as the bicipital groove, which can be narrowed by bony proliferation[33]. Although periarticular osteophytes have been regarded as pain generators, it is possible that they instead attempt to provide pain relief. Osteophytes and joint capsule thickening may serve as natural splints immobilizing a painful joint and potentially even leading to spontaneous arthrodesis.

Figure 5. Standard anterior-posterior radiograph of a primary glenohumeral osteoarthritis. Obliteration of the joint space and osteophytes in the antero-inferior aspects of the humeral head and inferior aspects of the glenoid are clearly visible.

Our understanding of the etiology of GHOA is derived from advancements made in understanding OA in general. Theories have evolved from age-related cartilage wear and tear to a disorder that affects the entire joint and its sur- rounding tissues. Some consider OA a common endpoint of a heterogeneous group of disorders that lead to degenerative joint damage[34].

Traditionally OA has been classified into primary (no known cause) and secondary (resulting from an identifiable cause) forms, but this dualistic division has been criticized. The pathogenesis of joint damage, seen as part of a common pathological process, is influenced by multiple factors [35].

These can be divided into non-specific and specific factors as well as into systemic and local factors. Joint damage develops from the interplay between these factors, where local or systemic factors, or non-specific or specific factors, may dominate[34,36]. Disease progression is, however, typically affected by a combination of genetic, behavioral, and environmental factors.

Non-specific systemic risk factors for glenohumeral joint damage include: advancing age[29], genetics[37-39], and obesity[40-42].

Excessive mechanical loading, heavy construction work and overhead sports are identified as non-specific local risk factors for glenohumeral joint damage[43-47].

Other athletes at risk of developing GHOA include weight lifters and throwing athletes such as baseball players[48].

1.2.1 **Specific Local Risk Factors for Glenohumeral Joint Damage**

1.2.2 ***Scapular morphology***. Several factors of scapular morphology have been associated with GHOA development. These include the lateral extension of the acromion as well as glenoid inclination. These two measurements have recently been combined to give the critical shoulder angle (CSA). Both a shorter acromion and a greater inferior glenoid inclination (leading to a lower CSA) result in

compressive forces by the deltoid muscle. This medially directed compressive force across the glenohumeral joint may lead to excess load- ing and subsequent OA[49].

Glenoid dysplasia, caused by abnormal development of the two ossification centers in the glenoid, is a further risk factor for GHOA. It is more com- mon in men and is characterized by hypoplasia of the infe- rior glenoid, often associated with glenoid retroversion, posterior joint wear, and humeral subluxation [50,51]. Once thought to be a rare condition, recent studies suggest glenoid dysplasia can be seen in 14% to 40% of shoulders[52]. Causes of dysplasia include idiopathic, familial or syndrome related. In addition dysplasia has been described in children with obstetric brachial plexus palsy[53,54]. Neuromuscular imbalance between internal and external rotators has in the past been suggested to be the primary cause of glenoid dysplasia[55]; however, direct damage to the ossification centers and internal rotation contracture may play a role. More recently, focus has shifted to neural denervation induced cellular alterations that lead to impaired bone growth, which has been shown to be a major factor in animal models[56].

1.2.3 ***Glenohumeral instability and instability repair.*** Prevalence of radiological GHOA changes—following both dislocations and instability surgery—have been reported as high as 56%– 68%, but symptoms are typically infrequent or mild[57-59]. Direct joint damage as well as altered biomechanics can be responsible for these radiological changes, but the degree to which these changes are caused by dislocation versus subsequent surgery is unclear. Although it is uncertain if laxity or joint instability per se is a risk factor for GHOA development, the association with shoulder dislocations (to which instability is a predisposing factor) has been established in numerous studies[57,58,60]. Patients with a single shoulder dislocation have a 10- to 20-fold increased risk of developing radiological GHOA 47 compared to persons without acute shoulder injuries[61]. Recurrent dislocations, older age at primary dislocation, and greater trauma energy further increase the risk of GHOA development[57-59].

1.2.4 ***Cuff tear arthritis.*** GHOA, due to traumatic or degenerative rotator cuff tears, displays three characteristic changes. These are rotator cuff insufficiency, cranial migration of the humeral head, and subsequent radiographic degenerative changes. Radiographs typically show bony erosion of the superior glenoid, resulting in acetabularization of the coracoacromial arch, and rounding off of the humeral greater tuberosity[62]. Cuff tear arthritis (CTA) is seen more commonly in women and mostly affects the shoulder of the dominant arm[31]. Hamada et al classified five evolutional grades of GHOA by analyzing radiographic findings of massive rotator cuff tears, in which the grades were presumed to reflect the temporal evolution of rotator cuff tears[63]. Briefly, the acromio-humeral interval (AHI) is maintained in Grade 1 and narrows in Grade 2. Acetabularization (concave deformity of the acromion undersurface) in addition to the Grade 2 narrowing is classified as Grade 3. In Grade 4, narrowing of the glenohumeral joint is added to the Grade 3 features, and Grade 5 comprises instances of humeral head collapse[63]. Subsequently, Walch et l divided Grade 4 of Hamada et al. into two subtypes: Grade 4A, glenohumeral arthritis without subacromial arthritis (acetabularization); and Grade 4B, glenohumeral arthritis with subacromial arthritis (Grade 4 of Hamada et al.)[64].

1.2.5 ***Milwaukee shoulder***. Milwaukee shoulder is a rare joint- destroying disease seen typically in older women that is associated with intra- and periarticular hydroxyapatite crystal deposition. Identification of these crystals by Alizarin Red staining is a hallmark of this rapidly progressive disease often showing marked erosion of the humeral head and surrounding soft tissues[65].

Additional specific local risk factors for GHOA are fractures[31] and humeral chondrolysis[66].

1.2.6 Specific systemic risk factors for glenohumeral joint damage

1.2.7***Inflammatory arthritis.*** Autoimmune mediated inflammatory causes include rheumatoid, psoriatic, and juvenile idiopathic arthritis, as well as spondyloarthropathies and systemic lupus erythematosus (SLE). Of these, rheumatoid arthritis (RA) is the most common, with more than half of patients showing involvement of the GH joint[67]. The worst affected patients typically have bilateral

disease and central glenoid wear patterns, but the associated pain may be more related to the inflammatory syno- vitis than the joint destruction itself. Crystalline arthropathies, including gout and pseudogout, caused by sodium urate and calcium pyrophosphate crystals in the synovial fluid, respectively, also lead to inflammatory joint destruction[31].

1.2.8 ***Avascular osteonecrosis***. Avascular osteonecrosis (AVN) of the humeral head leads to bony collapse and loss of joint congruity and has been estimated to account for 5% of all GHOA[68]. It is the second most common site of AVN following the hip[69]. Common etiological factors include trauma, corticosteroid use, and alcoholism, while rare causes include Gaucher disease, sickle cell anemia, Caisson disease, and certain pharmaceuticals[69].

1.2.9 ***Endocrine disease sand neuropathic arthropathy***

Neuropathic arthropathy, also known as Charcot arthropathy, is another rare degenerative disorder characterized by rapid destruction of the joint with extensive involvement of the bone and soft tissue. Cervical syringomyelia accounts for 75% of neuropathic shoulder arthropathy, while other causes of insensitivity, such as diabetes mellitus, chronic alcoholism, or end-stage renal disease, are less common[70]. The underlying pathophysiology is not well understood, but neurovascular and neurotraumatic theories have been developed, with the loss of nociception and proprioception playing important roles.

1.3: **Computed tomography evaluation of multiplanar glenoid deformity in osteoarthritis**

The classical computed tomography (CT) parameters describing the bony anatomy of the humerus and glenoid are two-dimensional (2D). They include the inclination and the version of the humerus and glenoid in the coronal and axial planes, respectively[71,72]. These values have a wide distribution, and therefore their use in the surgical setting is criticized. This broad distribution is related to both anatomical factors and positional errors[73,74]

One of the anatomical factors is the torsion of the glenoid from cranial to caudal. The positional factor means that the version of the glenoid can vary greatly with the position of the scapula on the CT-scan.

A three-dimensional (3D) CT-scan reconstruction and evaluation can overcome this shortcoming. When the measurements are performed between two bony structures, like in the glenohumeral joint, the positional influence of the scapula can be minimalized by standardizing the patients positioning in the CT-scan gantry. This position mimics the operative conditions and keeps the glenohumeral joint in a neutral position. So these two factors (3D reconstruction images and the standardized position of the patient in the CT-scan gantry) can reduce the variability of the anatomical measurement[75]. 3D anatomy of the glenohumeral joint enables improved geometrical fitting. A cut through the "humeral sphere" at the level of the collum anatomicum defines a circular plane unavailable via 2D imaging. The introduction of the "native" retroversion and inclination, guided by the anatomical neck of the humerus, improved the 3D restoration of the center of rotation (CoR)[76-78]. On the glenoid side, the classical parameters (angles between lines like retroversion and inclination), are still used because there is no consensus on which plane to restore. The fact that there is no consensus about which plane to use can be explained by the variability of the morphology of the glenoid. The glenoid has been described as comma, pear or teardrop, round, and ovoid-shaped[79]. Despite no reference plane having been described so far on the glenoid side, it is recognized that the inferior part of the glenoid constantly has the shape of a true circle[80,81]. The orthopedic surgeon tends to use the midpoint of the glenoid described as the

crossing line between the most superior and inferior point of the glenoid and the largest antero-posterior distance.

Research studies about the variability of the shape of the glenoid cavity, described that only the peripheral rim of the inferior quadrants of the articular surface of the glenoid was found to be located on a circle[80]. Furthermore, the definition of the center of this circle appeared to be more reliable than determining the center of the glenoid as the cross point of the cranio- caudal and antero-posterior axis of the glenoid. Finding the 3D mathematical center of the glenoid on 3D CT-scan reconstruction images seems to overcome this issue. The inferior glenoid plane (created with the most anterior, posterior and inferior glenoid point at the bony rim of the inferior glenoid) would provide the least variability in vivo and would be the most suitable for prosthetic surgery of the glenoid[75,80].

Walch et al previously developed a classification system to describe glenoid morphology in cases of primary glenohumeral osteoarthritis[82]. Since that classification system was first presented, several authors have commented on the interobserver and intraobserver reliability of the classification, with varying results[83-85].

The main limitation of the original Walch classification was the use of a traditional 2D CT scans, which have since been found to portray glenoid version less reliably than 3D reconstructions that analyze the scapula as a free body, as reported above[86-89].

The original classification includes 5 categories of glenoid patterns: (1) A1- centered humeral head, minor erosion; (2) A2—centered humeral head, major central glenoid erosion; (3) B1—posterior subluxated head, no bony erosion; (4) B2—posterior subluxated head, posterior erosion with biconcavity of the glenoid; and (5) C—dysplastic glenoid with at least 25° of retroversion regardless of erosion[82]. Bercik et al[90] proposed several modifications to this original classification system, suggesting the addition of the "B3" and "D" glenoids and a more precise definition of the A2 glenoid. They defined the B3 glenoid as monoconcave and posteriorly worn, with at least 15° of retroversion or

at least 70% posterior humeral head subluxation, or both. The B3 glenoid with posterior subluxation without significant retroversion differs from the B1 by the presence of posterior wear. They defined the D glenoid as one with any level of glenoid anteversion or with humeral head subluxation of less than 40% (ie, anterior subluxation). The definition of the A2 glenoid "cupula" was also updated to describe glenoids in which a line drawn from the anterior to posterior rims of the native glenoid transects the humeral head. This was in contrast to the A1 glenoid, in which a line drawn from the anterior to posterior rim of the native glenoid does not transect the humeral head. Lastly they clarified the C glenoid to be a dysplastic glenoid with at least 25° of retroversion "not caused by erosion" (Figure 6).

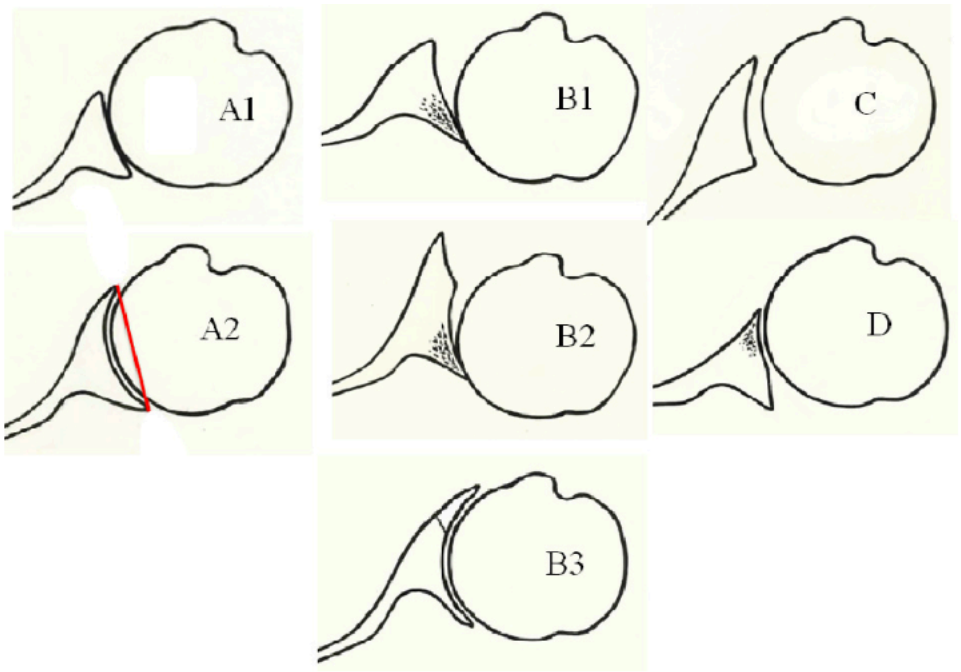

Figure 6. Representation of glenoid morphology in osteoarthritis according to Walch et al as modified by Bercik et al[90].

Recent studies have aimed to quantify the direction and amount of glenoid erosion using 3D reconstructions of CT scans. The transformations into 3 dimension is crucial for planning the correction of posterior glenoid bone loss and pathologic retroversion in order to restore the native joint line [91,92]. The use of 3D CT reconstruction allowed to identify the multiplanar glenoid deformity, and consequently the position of the implant components that prevent overmedialization of the joint line. 3D CT imaging can assist shoulder surgeons to choose between asymmetric reaming, glenoid bone grafting, and augmented glenoid components, to address excessive retroversion and glenoid bone loss[93-95].

Otto et al described three different patterns of multiplanar glenoid wear in type B2 biconcave glenoid[96]. They found that the most common pattern of erosion was in the posterior-central direction, with the remaining cohort falling into either the posterior-inferior or posterior-superior direction (Figure 7).

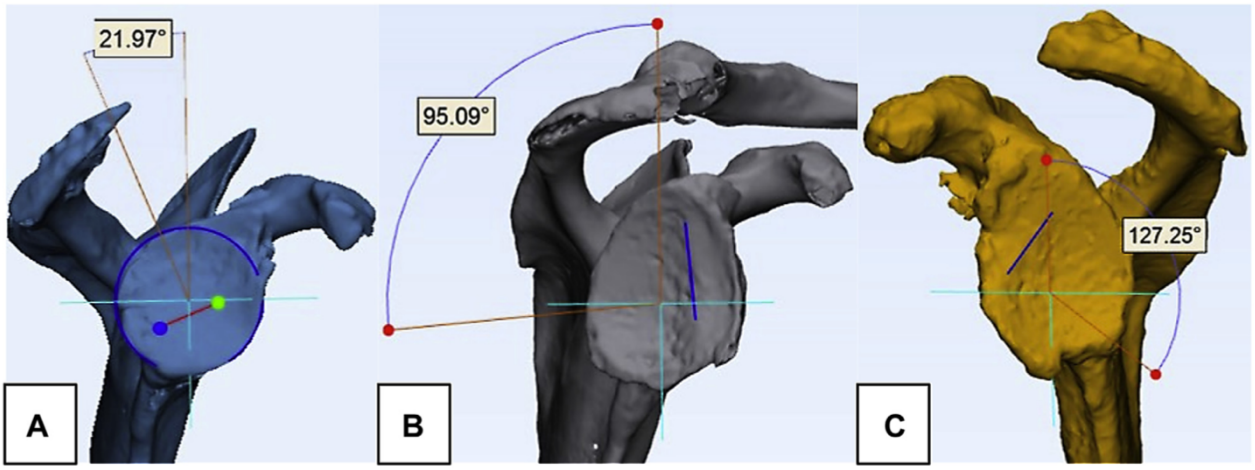

Figure 7. 3D CT representation of the erosion orientation in type B2 biconcave glenoids. A, posterior-superior, B, posterior-central, and C, posterior-inferior wear patterns[96].

Across all deformities, Knowles et al reported that the line of glenoid erosion in B2 glenoids was directed toward the posterior-inferior quadrant with the orientation of bone loss directed toward the 8-o'clock position; in addition, the radius of curvature for the neoglenoid was flatter than the paleoglenoid[92]. Otto et al found that the direction deviated in many cases from 8'oclock position[96]. Overall, this informations may assist surgeons in addressing technical factors associated with glenoid resurfacing of the B2 erosion pattern and manufacturers in the fabrication of implants that can better address commonly seen glenoid deformities.

The incidence of pathologic bone remodeling in the context of CTA is near 40%[97,98]. Superior glenoid wear is common in patients with CTA and results from progressive erosion of the glenoid by the superiorly migrated humeral head[97 99].

About 37.5% of patients with rotator cuff-deficient shoulders had some degree of glenoid wear, and more advanced CTA has been associated with superior glenoid wear[97,98]. Favard classified glenoid wear with rotator cuff tear arthritis based on the location and extent of erosion at the superior and inferior aspects of the glenoid[100]. Favard superior glenoid wear classification system includes types E0 (no glenoid wear), E1 (concentric erosion of glenoid), E2 (erosion limited to upper part of glenoid), E3 (erosion extending to inferior part of glenoid), and E4 (erosion predominantly located at inferior part of glenoid) (Figure 8).

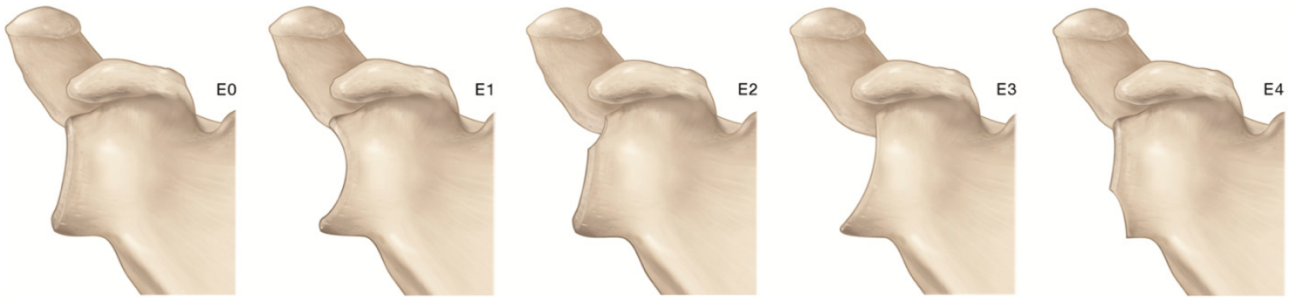

Figure 8. Representation of glenoid wear in cuff tear arthritis according to Favard et al[100].

Recently, Walch et al analyzed the CT 2D and 3D characteristic of E4 type glenoid deformity and they found anterior erosion and anteversion associated with anterior subluxation of the humeral head[101].

In order to the effects of GHOA on the surround musculature, recent research findings demonstrated that, contrary to what was thought, GHOA is not associated with deltoid atrophy and that increasing posterior deltoid areas was associated with glenoid retroversion in the Walch B-type glenoid deformity[102].

Overall, accurate and consistent positioning of the baseplate of a reverse shoulder arthroplasty(RSA) within acceptable limits of version and inclination should be achieved to ensure functional tension on the deltoid muscle and other soft tissues[103,104].

1.4 **Brief history of shoulder arthroplasty in osteoarthritis**

The first prosthetic shoulder arthroplasty performed has been ascribed to the French surgeon Jules Emile Péan in 1893 who implanted a platinum and rubber replacement in a a 37-year- old baker. The patient reportedly had increased strength and ROM, but unfortunately, the infection recurred, requiring removal of the prosthesis 2 years later[105]. The development of the procedure came in the 1950s when Neer described the results using a vitallium prosthesis to treat comminuted fractures of the head of the humerus[106]. Although pain relief was reliably obtained with hemiarthroplasty, Neer reported variable strength and function in patients with irreparable rotator cuff tears[106]. About 20 years later, and with the addition of a glenoid component, he described a total shoulder replacement (TSR) for the treatment of GHOA[33]. Since then, there has been a progressive improvement, culminating in the concept of anatomical reconstruction of the proximal humerus in the early 1990s, when the size and design of the humeral component were reconsidered[76,107-109]. Unconstrained prosthesis of the shoulder is now used widely to treat GHOA with good and reproducible results. The outcome after the use of unconstrained prostheses in complex fractures of the proximal humerus and in CTA has been less predictable. Although good relief from pain has usually been obtained, most patients had a limited range of movement, leading to difficulties with the activities of daily living. These poor results led to the development of specific implants for these difficult problems, a low-profile prothesis for fractures and a semiconstrained reversed-geometry design for arthritis resulting from a tear of the cuff[110-113]. Dislocation and scapular fixation remained a concern with this implant[114] and Neer remained convinced rotator cuff repair, not constraint, was essential for improved shoulder function. His Mark III prosthesis was therefore abandoned, although others continued to explore the reverse shoulder concept. Similar negative biomechanical effects were reported with several reverse implant systems developed beginning in the 1970s with variable designs for scapular fixation [112]. The system created by Paul Grammont in 1985 differed from previous reverse shoulder arthroplasty (RSA) concepts in that

Grammont's system focused on four keys features[111]: (1) the prosthesis must be inherently stable; (2) the weightbearing part must be convex, and the supported part must be concave; (3) the center of the sphere must be at or within the glenoid neck; and (4) the center of rotation must be medialized (Figure 9).

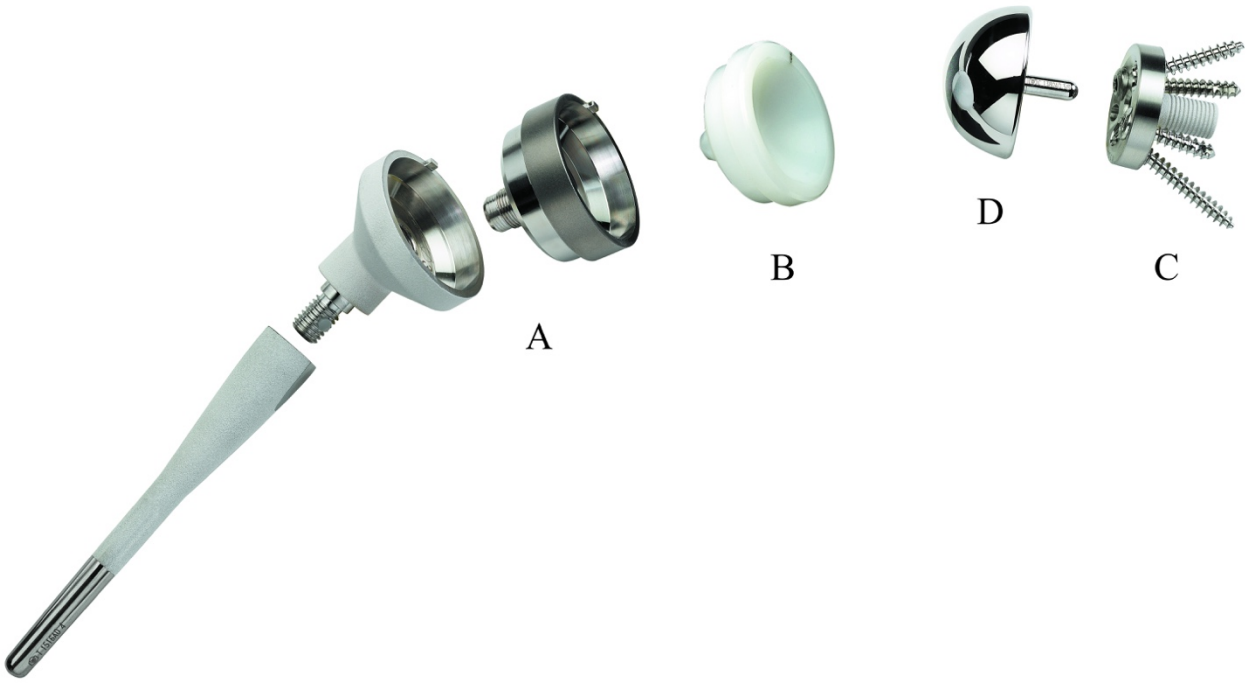

Figure 9. Grammont reverse design of shoulder arthroplasty. The humeral component included: A) a distal stem with a metaphysis and an optional humeral spacer; B) a centered (standard), and retentive constrained humeral insert, with variable height (+ 6 mm, + 9 mm, and + 12 mm). The glenoid component included: C) a hydroxyapatite-coated baseplate (25 and 29 mm) with a central post and 4 self-tapping screws (2 compression screws and 2 multidirectional locking screws); and D) centered and eccentric (+ 2 mm and + 4 mm) glenospheres.

Grammont noted the deltoid function could be increased by moving the CoR distally and medially in comparison to the native glenohumeral articulation. The system created by Paul Grammont opened the way for the modern and functional RSA.

1.5 **Design of shoulder arthroplasty**

1.5.1 **Anatomic implants**

Anatomical total shoulder arthroplasty (TSA) make use of unconstrained monoblock (Fugure 10) or modular humeral components (Figure 11 A-B). Recent stemless modern implant fixed in the humeral metaphysis are market available.The last generation of humeral component are the short stem, provided of a prevalent methaphysal grip (Figure 12). Head prostheses are available in several size, standard or with eccentric offset[115].

Figure 10. Monoblock humeral component with offset head prosthesis of total shoulder arthroplasty.

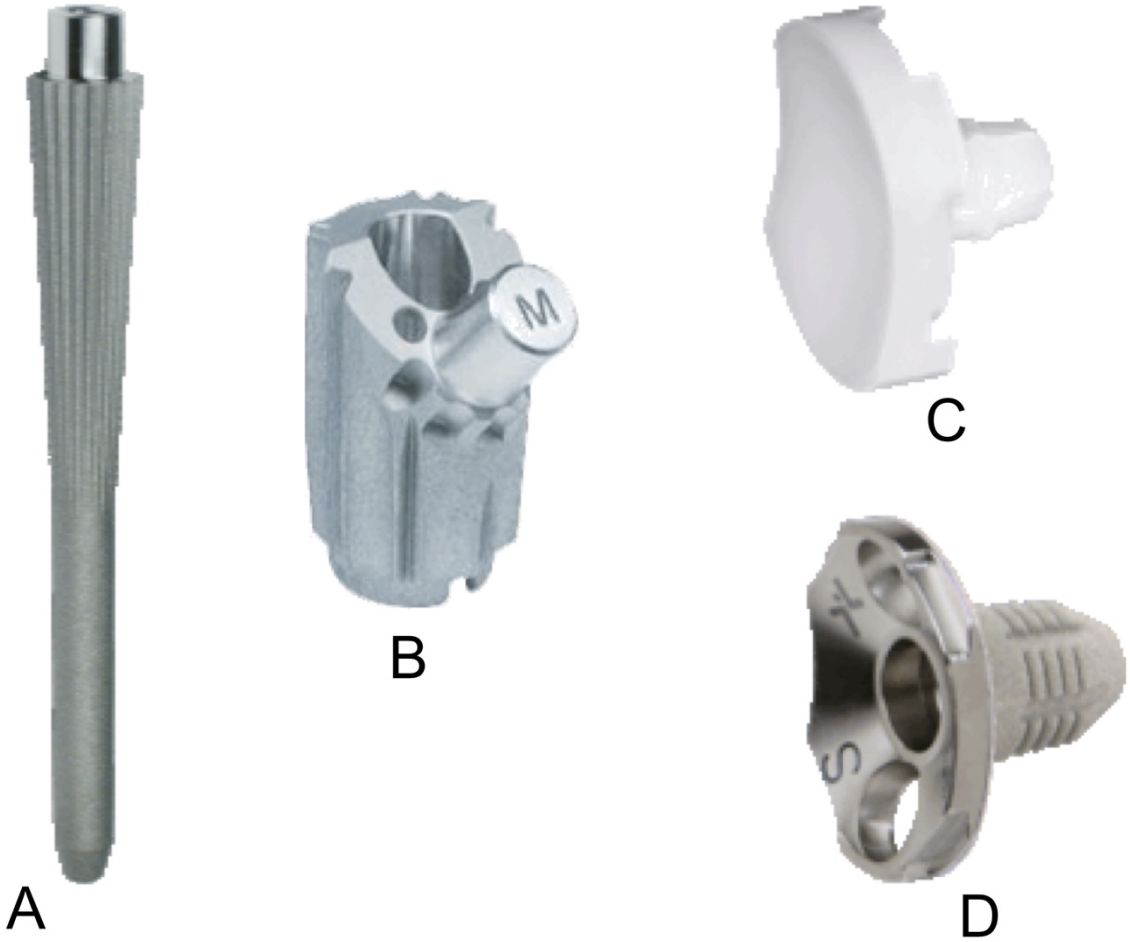

Figure 11. Moduar system of total shoulder arthroplasty. A, standard stem; B, humeral body; C, polyethylene liner; D, metal backed glenoid component.

Figure 12. Curved short stem humeral components (standard press fit and titanium coating) with offset head prosthesis.

Glenoid prostheses include:

1. polyethylene components with keel or pegs, fixed in the cancellous bone with cement[116]; the pegged glenoid are also available with a flanged uncemented central peg to promote osseointegration[117,118] (Figure 13 A)
2. standard metal-backed glenoid fixed with screw and covered with a polyethylene liner[119] (Figure 11 C-D)
3. trabecular tantalium-backed glenoid (TM®) fixed in the bone under pressure[120] (Figure 13 B). As for the glenoid, a TM® humeral component enabling the healing of the humeral fractures is available[121].

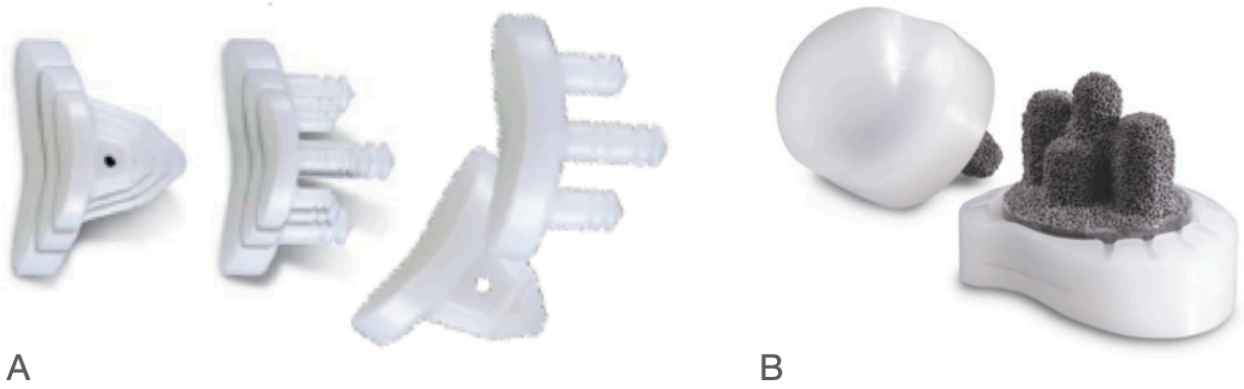

Figure 13. Glenoid components of total shoulder arthroplasty. A, pegged and keeled polyethylene component; B, trabecular tantalum backed (TM®) component.

1.5.2 **Reverse implants**

Reverse prostheses is a semiconstrained totally modular device (Figure 9). The glenoid component consist of a baseplate (metaglene), provided with a large central peg and secured to the native glenoid by cortical screws (2 or 4), which may be straight or angled, on which is fit the glenosphere (a rounded metal ball approximately two third of sphere) that is attached to the baseplate with a screw. The glenosphere can be completely medialized or slightly lateralized, to prevent scapular neck erosion. The humeral component consists of a proximal cup-shaped portion and a metal stem to be press-fitted or cemented in the medullary canal. A radiolucent polyethylene insert sits in this cup portion and articulates with the glenosphere. As for the anatomical implants, also for reverse prostheses are available short stem having a predominantly metaphyseal grip (Figure 14).

Figure 14. Short stem lateralized humeral component of reverse shoulder arthroplasty. A) a hydroxyapatite-coated curved short stem 132.5° inclination; B) an eccentric (+ 1.5 mm and + 3.5 mm) reverse tray; and C) an asymmetric polyethylene insert (thickness + 6 mm and + 9 mm) with 12.5° inclination.

1.5.3 **Biomechanics**

1.5.4 **Anatomic arthroplasty**

Satisfactory results of shoulder replacement require: a) prosthetic reproduction of a normal bone morphology 2) restoration of capsular tension 3) restoration of the stabilizing and motor function of the muscle. Geometric parameters that we have to consider when we perform a shoulder arthroplasty include: i) neck inclination, ii) humeral head diameter and height, iii)humeral head retroversion, iv) head offsets, v)acromion-humeral distance.

The cervico-diaphyseal angle measures between 135° and 145°[122]. Prostheses are usually designed with a fixed angle of 130°-135° and the instrumentations perform head osteotomy at that angle. The diameter of the humeral head[15] varies widely from 38 to 58 mm (median 46 mm). Degenerative diseases altering the spherical shape so the prosthetic head diameter often cannot be determined. The component's diameter is thus chosen at the time of trial reduction based on the height of the hemisphere that has a broad linear relationship with the diameter of the head. In all humeri the superior edge of the head protrudes above the superior edge of the greater tuberosity by 2-5 mm[123]. When the head component is positioned under the edge of the greater tuberosity, the joint's instantaneous centre of rotations descends, resulting on reduced lowering of the humeral head and increased tension in adduction, and signally, in early, painful subacromial impingement. On the other hand, a head protruding excessively above the greater tuberosity induces increased tension on the cuff ("overstuffing"). The humeral head is retroverted with respect to the coronal plane. The angle of retroversion is the subtended between the epicondylar axis and the central axis of the humeral head. Its median values is 20° and it is proportional to the angle of retroversion of the scapula which instead is widely variable (0°-60°). Small errors in head retroversion do not significantly influence the tension of the caspulo-ligamentous system nor the instantaneous CoR; an excessive retroversion may induce posterior head subluxation in case of a posterior cuff tear, whereas an insufficient retroversion may

cause subscapularis impingement. The center of the head does not lies on the diaphyseal humeral axis, but is displaced both in the coronal and the transverse planes. In the coronal axis the offset ranges from 2 mm to 12 mm (median 7 mm) (medial and lateral offset); lower values results in a looser capsuloligamentous complex, while excessive values produce overstuffing and possible joint stiffness. The center of the head lies 0-10 mm (median 4 mm) posterior to the diaphyseal axis (posterior humeral head offset)[76]. When this features, and the instantaneous CoR, move anteriorly induce an abnormal contact with the glenoid and abnormal pressure on the subscapularis. The space between humeral head and acromion is about 2 cm. A wider space reduce muscle tension and produce loss of strenght in elevation while a narrower spacer result in a stiffer joint and possibly subacromial impingement.

1.5.5 **Reverse arthroplasty**

The principles of the Grammont' reverse design, as previously described, were inherent prosthetic stability, convexity of the glenoid component, glenosphere center at or within the glenoid neck, and a medialized and CoR [124]. In presence of rotator cuff insufficiency, reverse arthroplasty prevent humeral proximal migration because with its congruent articulating surface achieve concentric motion. In fact, unlike total anatomic arthroplasty, that has a shallow glenoid component which cannot resist proximal migration and dislocation if the deltoid force vector is greater than 30° from the centerline, Grammont reverse arthroplasty has a non-anatomic neck-shaft angle (NSA) of 155° and the resultant deltoid force vector can subtend an angle of at least 45° from the centerline without risk of dislocation[125,126]. The medialization of the CoR at or medial to the prostheses-bone-interface, contributed to avoid the problem of early loosening of the first reverse implants, because it reduced the shear forces and increase compressive forces, but the consequence was that humeral adduction caused inferior impingement, fostering the scapular neck erosion ("scapular notching")[100]. The location of the CoR affects the shoulder range of motion (ROM) and the lever arm of the deltoid[127].

With the inferior baseplate positioning and the CoR medialized the lever arm lenght is doubled and as a consequence the efficacy of the deltoid for abduction is approximately doubled, but at the same time deltoid excursion produces a lesser arc of motion[127,128]. For these reasons most of the surgeons using Grammont design of RSA tend to position the glenosphere inferiorly and slight laterally, because it has been shown that maximize the free-impingement arc of motion and increase the ROM in abduction[129].

The main modification of the Grammont design directed to reduce the risk of scapular notching was the lateralization of the CoR. This change can be performed at the level of the baseplate, with bone or metallic increased offset implants (bony-increased offset RSA [BIO-RSA] and metallic-increased offset. RSA [MIO-RSA])[130], or at the level of the glenosphere, changing its design[131]. Lateralization of the CoR away from the glenosphere/glenoid interface increases the risk of mechanical loosening.

Changes of NSA, from 155° to 135°, and the new position of the reverse tray in onlay configuration, have produced a novel stem geometry that preserve the tuberosities, and the insertion of the rotator cuff (RC) (if present), with potential effects on external rotation recovery[132] (Figure 10).

1.5.6 **Criteria for anatomic and reverse arthroplasty**

Conventional TSA is indicated in patients with concentric shoulder osteoarthritis[116]. In cases of arthritis with instability derived from humeral head deficiency, the prosthetic humeral component can restore the full articular surface. Glenoid prostheses can restore the contour of arthritic glenoid provided that the bone beneath ensure adequate support[125,126]. When shoulder osteoarthritis is associated with instability from rotator cuff tears, conventional arthroplasty and rotator cuff repair may guarantee joint stability. Arthritis following instability with excessive capsular laxity can be treated with anatomical arthroplasty with larger humeral head and capsular tightening[125-127]. Even in cases with cuff deficiency and upward migration of the humeral head stabilized by an intact coracoacromial arch, with an efficient deltoid, humeral hemiarthroplasty may a sufficient shoulder function[125,126], especially in young patients with high functional demand where reverse arthroplasty is at risk of failure. Conventional arthroplasty is contraindicated to treat instability with unreconstructable soft-tissue or osseous deficiencies, such as severe posterior glenoid bone deficiency. Even in case where the posterior capsule and rotator cuff have been lost after trauma or previous surgery, conventional arthroplasty cannot restore posterior stability[125-127]. Mechanical criteria for RSA include having a functional deltoid and being able to achieve stable glenoid baseplate fixation. Traditionally, RSA was performed for glenohumeral arthritis in elderly patients with rotator cuff insufficiency, massive cuff tear with arthritis and massive irreparable cuff tear[127,133]. However, the poor results observed in some indications with unconstrained total shoulder arthroplasty (TSA) persuaded most surgeons to extend the use of RSA also to inflammatory arthritis, static humeral instability, sequelae or post-traumatic arthritis in cases of nonunion or severe malunion of the greater tuberosity, revision of failed anatomical arthroplasty[127,128,134,135]. The semi-constrained nature of RSA confers inherent stability to the construct, while screw fixation of the glenoid baseplate allows easier incorporation of bone graft in cases of bone loss. The role of RSA in cases of severe glenoid bone loss has been limited to elderly, low-demand

patients. The semi-constrained nature of RSA components, while offering beneficial stability, also raises questions about implant longevity. With limited follow-up available, several studies have focused on the incidence and implications of scapular notching to evaluate early implant performance.

1.5.7 **Published evidence of glenoid lateralization with bone or metal augmented baseplate in RSA**

Management of severe glenoid erosion with RSA requires extensive reaming to restore the native retroversion and inclination, which increases the risk of glenoid medialization and subsequent failure of baseplate fixation[136 137,138, 139, 140-143]. The use of autologous bone graft harvested from the humeral head and fixed on the baseplate at the interface of the native glenoid, was proposed to minimize glenoid reaming and restore glenoid bone stock (Bony-Increased Offset, BIO- RSA)[144]. The authors described the humeral head autograft as symmetrical (BIO-RSA) or asymmetrical (angled BIO-RSA), in relationship to the orientation of glenoid deficiency.

Boileau et al demonstrated satisfactory early and long-term outcomes of BIO-RSA in shoulder osteoarthritis, with radiographic evidence of good graft incorporation[93]. However, other studies highlighted a higher rate of graft resorption, scapular notching and baseplate loosening, thus creating concern about the effectiveness of this procedure[145]. Metal augmented glenoid components (Metal-Increased Offset – MIO-RSA) have been proposed as viable alternative to BIO-RSA, preserving more native bone stock and restoring the joint line, with a final goal of increasing the baseplate support[143]. Researchers supporting the BIO-RSA have criticized metal augmented glenoid components, because they would not allow a multiplanar correction and reconstruction of glenoid bone stock[93]. However, recent clinical investigations have encouraged the use of MIO-RSA, reporting satisfactory clinical outcomes , and have also demonstrated their ability to correct the glenoid deformity[140,146,147]. The choice of bone or metallic augmentation is particularly important in type E2/E3 and B2/B3 glenoid deformities, where the patho-anatomic feature and erosion orientation require higher volume of bone removal using standard baseplate design[143,148]. Radiographic features of a globally lateralized RSA[130,149] are described in the figure 15. A recent randomized clinical trial, comparing BIO-RSA and

metal augments in RSA with curved onlay-humeral component, demonstrated that both systems provide stable initial fixation and similar clinical outcomes[147].

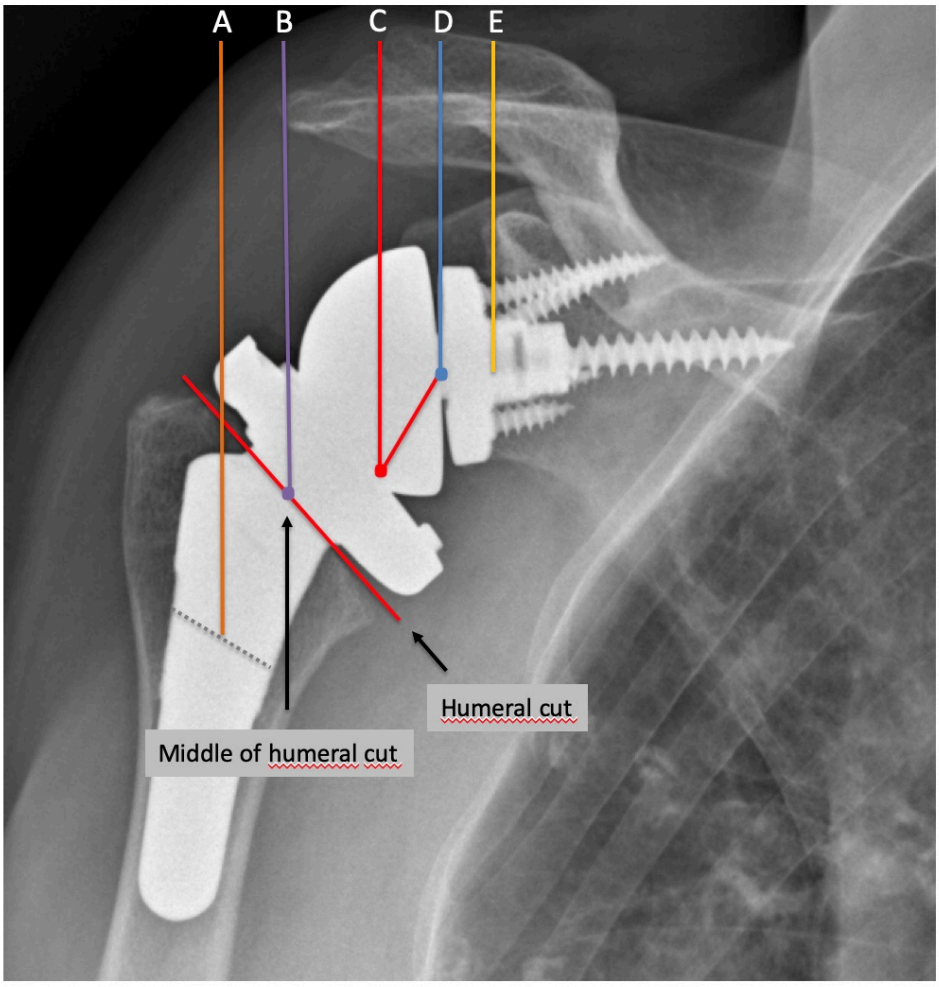

Figure 15. Radiographic references to measure humeral and glenoid offset in lateralized RSA (global lateral offset), as reported by Merolla et al[130] in line with the criteria described by Werthel et al[150]. Line A is the vertical line passing through the middle of the diaphysis of the humeral stem. Line B is the horizontal line passing through the middle of the surface of the humeral implant at the level of the humeral cut. Line C is the vertical line passing through the "pivot point" defined as the deepest point of the articular surface of the humeral insert measured perpendicular to the surface of the humeral insert. Line D is the vertical line passing through the centre of rotation of the joint. Line E is the vertical line passing through the bone-glenoid baseplate interface. Humeral lateral offset (distance AC) was defined as the sum of the humeral stem offset (distance AB) and of the humeral insert offset (distance BC).

Glenoid lateral offset (distance CE) was defined as the sum of the "perceived radius of the glenosphere" (distance CD) and of the centre of rotation offset (distance DE).

CHAPTER 2

Objectives

Objectives of this study were to compare clinical and radiographic outcomes of BIO-RSA and MIO-RSA in a large cohort of patients. We tested two hypotheses: i) metal augmented baseplate give similar clinical outcomes and rate of scapular notching, and prevents the medialization of the joint line similarly to BIO-RSA; ii) bone graft viability and healing in BIO-RSA patients are impaired over time, thus making concern about baseplate fixation and stability in the long-term.

CHAPTER 3

Materials and Methods

This was a retrospective analysis of data collected from Januray 2016 to December 2018. It involved 84 consecutive patients who underwent RSA with glenoid lateralization using bone (BIO-RSA group) or metal augmented baseplate (MIO-RSA group). Two different glenoid implant models were used: Aequalis Ascend™ Flex Reverse II in BIO-RSA group and Aequalis Ascend™ Flex Perform® in MIO-RSA group (Wright Medical, Memphis, Tennessee, USA). Both groups had the same curved-stem with onlay-humeral component. The study was performed in two orthopedic units (Shoulder and Elbow Unit of "Cervesi" Hospital, Cattolica – Italy -, and the Orthopaedic and Trauma Unit, University Hospital, Modena - Italy) and was approved by the institutional review board of coordinator center as part of a larger Shoulder Arthroplasty investigation (prot. n. 6478/2019 I.5/117). Patients with a preoperative diagnosis of primary osteoarthritis (OA) or cuff tear arthropathy (CTA) and a minimum follow-up of 24 months were included. There were no specific exclusion criteria. A power analysis was performed considering a 1.7 point difference in the Western Ontario Osteoarthritis of the Shoulder (WOOS) Index between the groups, a standard deviation of the score of 1.8 points, and a minimal clinically important difference (MCID) of 0.4 points. Using these parameters and a power of 0.8, a sample size of at least 44 subjects (22 per group) was required. Of the 84 patients who were invited, 1 declined to participate because of logistic problems and 2 had incomplete clinical and radiographic data, leaving 81 patients (83 shoulders) in the study with complete clinical and radiographic data. The demographics and perioperative data of both the study groups are reported in Table 1.

Variable	BIO-RSA	MIO-RSA	P value
Shoulders (n°)	44	39	0.391
Gender, F/M (n°) (%)	31/13 (70/30)	18/21 (47/53)	*.02*
BMI	27.6 (23-38)	24.0 (17-31)	*.0002*
Age (years)	71.6 (50-86)	67.0 (37-82)	.0485
Preoperative diagnosis			.370
Primary OA	25 (56)	22 (57)	0.370
CTA	19 (44)	17 (43)	0.167
Glenoid morphology in primary OA*			.335
B1	2 (7)	2 (7)	
B2	17 (72).	16 (73)	
B3	5 (18)	4 (20)	
C	1 (3)	0	
Superior glenoid erosion in CTA**			0.370
E1	1 (3)	1 (5)	
E2	10 (50)	9 (55)	
E3	8 (47)	7 (40)	

Table 1. Demographics and perioperative data of the 2 groups of patients.

BIO-RSA: bony-increased offset reverse shoulder arthroplasty.

MIO-RSA: metallic-increased offset reverse shoulder arthroplasty.

*Glenoid arthritis was classified according to the criteria of Walch et al as modified by Bercik et al for primary osteoarthritis[90].

**Superior Glenoid erosion was graded according to Favard et al[100]

Significant value is in italic.

3.1 Preoperative imaging and computerized 3D planning

Plain radiographs in anterior-posterior (AP) Grashey, outlet and axillary views were performed in all the cases. Glenoid morphology and wear were assessed by CT scans and classified according to established criteria for primary OA[90] and CTA[151]. Rotator cuff fatty infiltration was assessed according to Goutallier et al[152]. Preoperative computerized 3D planning was performed in all cases by using the Blueprint software (Wright Medical, Edina, MN, USA) by two operating surgeons. All files were exported in an automated software program (Glenosys) for 3D assessment. It allows an automated segmentation of the humerus and scapula, definition of scapular planes, determination of glenoid version and humeral head subluxation[153]. The version angle is automatically computed as the angulation between the scapular plane and the glenoid best-fit sphere centerline projected on the transverse scapular plane (Figure 16).

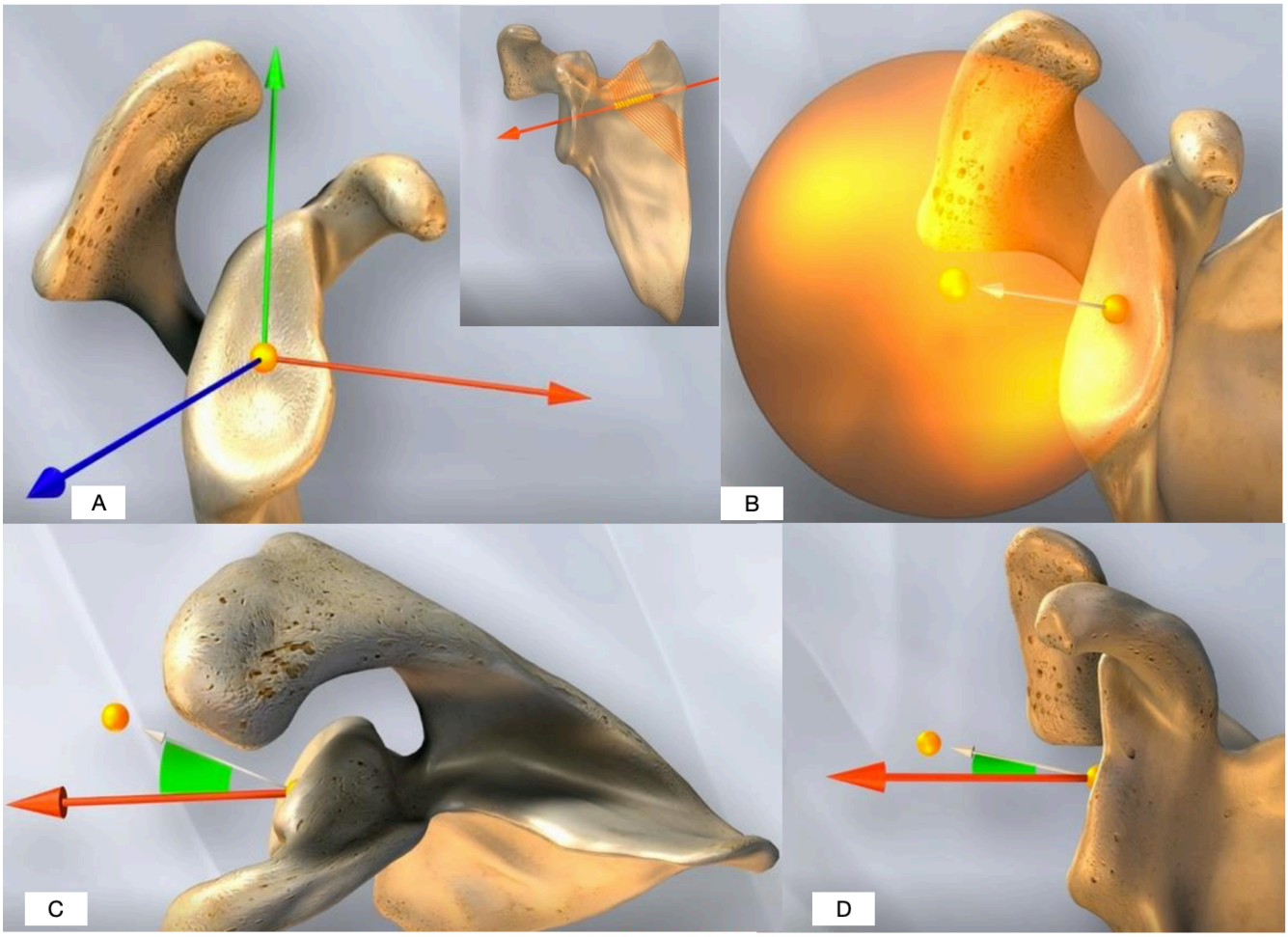

Figure 16. Preoperative 3D software planning used in this study. The system automatically 3D segments CT scan series. A) an orthogonal coordinate system is created after a previous identification of scapular and transverse axes, B) the software then extrapolates a best-fit sphere from the articulating data points, where a radius is drawn from the center of the best fit sphere to the center of the glenoid, C) glenoid version is identified in the axial view as the angle between the transverse axis and the radius of the best fit sphere in the anterior-posterior direction, D) glenoid inclination is identified in the coronal view as the angle between the transverse axis and the radius of the best fit sphere in the superior-inferior direction.

The direction of glenoid erosion was recorded as posterior-superior, posterior-central and posterior-inferior.

The orientation was reported as the angle between the glenoid centerline and the transverse axis. Humeral head subluxation was described as the percentage of the part of the humeral head posterior to the scapular plane. The parameters selected by surgeons during the planning helped to find an implant configuration and position that would maximize joint motion and minimizes scapular notching of the humeral component. Preoperative templating was carried out for each implant, but the final size and placement of the prosthesis was evaluated intraoperatively.

3.2 Implant design and configuration

We used different glenoid components in the two study groups. The BIO-RSA group had a standard 29-mm baseplate with a conical central post (standard 15 mm or extralong 25 mm) and 4 peripheral screws. The MIO-RSA group had a porous titanium augmented baseplate in different diameters (25 mm and 29 mm) and configurations (half wedge [35°] and full wedge [15°]) (Figure 17). The glenosphere had 2 diameters (36 or 42 mm) and included a standard centered and lowered eccentric type (+2 mm) with both implants.

Figure 17. Augmented baseplate used in this study. A, half wedge baseplate (35°, 29 and 25 mm); B, full wedge baseplate (15°, 29 and 25 mm).

The humeral component of both implants had a short, curved, monoblock stem and 2 types of eccentric reverse tray (low offset, 1.5 mm; and high offset, 3.3 mm) of variable thickness (+ 0 mm, + 6 mm, + 12 mm). Polyethylene (PE) inserts of different thickness (+6 mm and +9 mm) could be used with this implant. The position of the offset tray influences the position of the humerus relative to the scapula. The surgeon's choice of tray eccentricity affects humerus lateralization and the acromiohumeral interval (arm lengthening). A 145° NSA, as systematically used in this study, is obtained using a stem inclination of 132.5° combined with an asymmetric 12.5° PE insert (Figure 14).

3.3 Clinical evaluation and outcome measures

Clinical status, active range of motion (ROM), and the Italian version of Western Ontario Osteoarthritis of the Shoulder (WOOS) index (score expressed as decimal from 0 [worse] to 1 [best])[154] were assessed pre-operatively and at the last follow-up visits. Active ROM was assessed in terms of forward elevation (AFE), lateral elevation (ALE), external rotation (ER; with the patient standing) using a goniometer, and internal rotation (IR; the ability to reach different levels of the spine with the thumb). The ROM and clinical scores were calculated by an examiner who did not participate in the surgical procedures.

3.4 Operative technique

Surgical procedures were carried out under general anesthesia along with an interscalene block, with the patient in beach chair position using a standard deltopectoral approach. If present, the long head of the biceps tendon underwent tenodesis. The subscapularis was detached by means of lesser tuberosity osteotomy or tenotomy.

Humeral preparation was identical in both the groups. Humeral head was resected at the level of the anatomic neck. The humeral canal was first sized , then the metaphyseal bone was compacted and preserved by the use of the compactors, progressively reaching the adapted size with rotational stability of the trials. Finally, the surface planer ensured adequate contact between the tray and the humeral cut. A cemented stem was required in 3 shoulders (4.3%) because of poor bone stock or insufficient rotational stability. The eccentric humeral tray was positioned so as not to exceed the level of the greater tuberosity. The thickness of the PE liner was 6 mm in all the cases. We consistently used an angle B of 132.5° with a 12.5° PE insert to reach the final 145° neck-shaft inclination.

Glenoid component in the BIO-RSA group was implanted using the technique described by Boileau et al[144]. A 29-mm circular glenoid guide was placed flush with the inferior border of the glenoid, and a 2.5-mm threaded wire was inserted into the glenoid vault with a 0° or a 10° inferior tilt (in shoulders in which the native glenoid had a superior orientation). The glenoid was reamed to abrade and flatten the surface as far as the subchondral bone (approximately 5 mm). An 8-mm central hole was drilled and the baseplate was impacted. A bone graft with a thickness of 7-10 mm was harvested from the humeral head and shaped on the baseplate to match the glenoid defect (posterior or superior). The baseplate with the graft was finally fixed using a long 25 mm central post (25 mm) implant, two compression, and two locking screws (Figure 18).

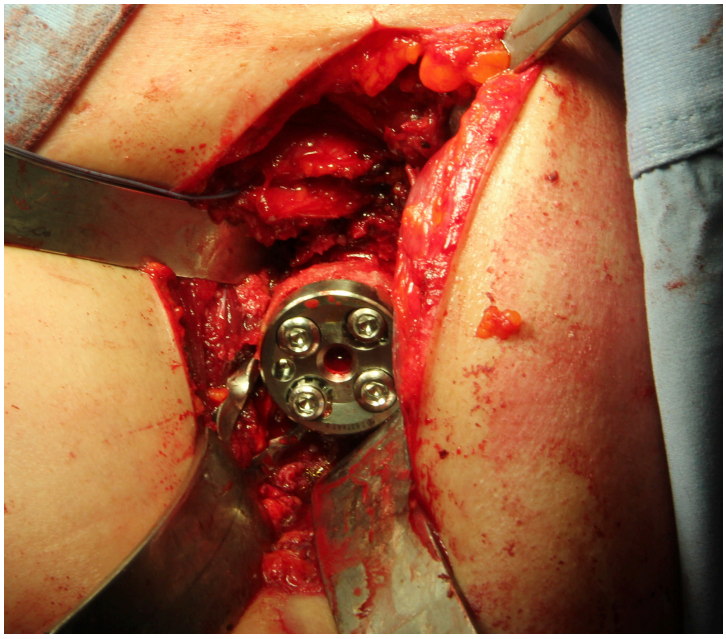

Figure 18. Intraoperative findings of BIO-RSA showing the baseplate with the autologous bone graft fixed with a long central post and peripheral screws.

The glenoid preparation in the MIO-RSA group followed manufacturer's recommendations. Anatomical pin guides of different sizes (small, medium, large and extra-large) and inferior inclination (0° or 10°) were used to fix the pin followed by reaming of the glenoid to obtain a flat surface.

After the paleo surface of the glenoid was adequately prepared, we reamed the defected/augmented/grafted bone or the neo portion of the glenoid with an augment reamer. An augmented trial of appropriate size, was used to evaluate if proper neo reaming was achieved. We drilled the hole for the baseplate post and the central screw and we chose the final baseplate according to the reamed glenoid surface (25 or 29 mm, full wedge augment 15°). The final central screw (6.5 or 9 mm diameter) was chosen according to the measured length using the central screw depth gauge followed by insertion of the the assembled baseplate which was fixed with four peripheral screws as previously described. The glenosphere was fixed to the base- plate using a Morse taper and a countersunk set screw.

The glenosphere diameter (36, 39 or 42 mm) was selected according to the humeral size and on the surgeon's decision. An eccentric glenosphere (+2 mm) was implanted in 12 shoulders of the BIO-RSA group and in 4 of the MIO-RSA group. Size of the baseplate, size and eccentricity of the glenosphere, length of the screws and size of the humeral component matched with that of measured in preoperative software planning in 95% of the shoulders.

The humerus was prepared with bone compactors, beginning with tools that were 3 or 4 sizes smaller than the sounders. The "twist test" was used to assess fixation, and stem size was selected on the basis of the size of the last compactor. The appropriate offset reversed tray (+0, +6, or +12 mm) was then chosen and assembled with the definitive stem. Finally, we placed the reversed PE insert on top of the reversed tray, carefully aligning the notch on the inserter with the lateral notch of the stem. The joint was reduced using a reducer, and prosthesis stability was checked.

3.5 Postoperative rehabilitation

After surgery, the arm was immobilized in a simple sling for 3 weeks. Our protocol includes initiation of passive motion in the scapular plane after 1 day postoperative. Active mobilization was allowed after 4 weeks, also including external rotation mobility. Active mobilization in internal rotation initiated after 5 weeks and strength exercises begun at 6 weeks.

3.6 **Postoperative imaging**

Standard radiographs were obtained in the immediate postoperative period and at the last follow-up evaluation. Radiologic changes around the reverse implants were assessed using previously reported criteria for the curved short stem humeral component (radiolucency, condensation lines, cortical thinning, spot weld, subsidence and resorption of the tuberosities, loosening) and the glenoid component (radiolucent lines in 5 zones, scapular notching, formation of bone scapular spurs, heterotopic ossifications[HO], and loosening)[132].

Healing of bone graft was assessed by recording any radiolucent lines and their size (mm). Thickness of the bone graft was evaluated in axillary or AP views according to the orientation of glenoid bone loss and the position of the asymmetrical graft. Any changes in bone graft thickness (expressed in mm ± standard deviation [SD]) were recorded comparing early and last postoperative radiographs.

Glenoid radiolucent lines assessed at the interface "glenoid bone-metal" of MIO-RSA explained the baseplate seating (no radiolucent lines: perfect seating; radiolucent lines < 2 mm: incomplete seating; radiolucent lines > 2 mm: loosening) in line with a previous study [155].

AP view were used to determine the vertical position and inclination of the glenosphere (global glenoid inclination) as measured by the **β** angle[93,156]. Vertical position of the glenosphere was assessed as described by Boileau et al[157].

Postoperative glenoid version was measured on axillary view according to Ho et al[158], modified for reverse shoulder arthroplasty

A blinded observer, who did not take part in the surgical procedures, reviewed the radiographs and also assessed any scapular fractures according to Crosby et al[159].

3.7 Statistical analysis

Descriptive statistics (absolute and percentage frequency, mean, median, SD, and range) for each group were calculated for all variables. Delta scores were calculated for clinical scores as the difference between postoperative and preoperative values. The preoperative scores and delta scores of the 2 groups were compared using the Mann-Whitney test. The possible association between each group and the qualitative variables, either baseline or postoperative, were analyzed with 2 Pearson χ test. The level of significance was set at 0.05. All analyses were performed with Stata Intercooled 9.2 software for Windows (StataCorp LP, College Station, TX, USA).

CHAPTER 4

Results

There were no differences in sample size, grade of preoperative glenoid arthritis (Walch and Favard classification), and rotator cuff fatty infiltration between the groups. BIO-RSA patients were slightly older ($p = 0.048$), had higher body mass index (BMI) ($p = 0.0002$) and higher percentage of females ($p=0.02$). Mean follow-up duration was 33.4 months (SD: 9.1) in the BIO-RSA group and 35.9 months (SD: 5.8) in the MIO-RSA group (Table 1).

4.1 Preoperative CT planning and measurements

Distribution of preoperative pattern of glenoid erosion is described in Table 1. Software planning found a median preoperative glenoid retroversion of 20° (range 17.5°-22°) in the BIO-RSA group and 16° (range 11°-18°) in MIO-RSA group ($p <0.001$). Glenoid inclination was similar in the two group, with a median of 11° (range 4.5°-13.5°) and 9° (range 4°-12°) in the BIO-RSA and MIO-RSA group, respectively. The rate of posterior humeral head subluxation was 76% (SD:5) in B2 glenoids and 78% (SD: 6) in B3. The direction of erosion was posterior-central and posterior-superior in 91% of B2 and 90% of B3 glenoids. The mean orientation was 21° and 22° in B2 and B3 glenoids, respectively. The direction of erosion in Type E2 and E3 glenoids was posterior-superior, with a rate of posterior humeral head subluxation of 74% (SD: 4%) .

4.2 Clinical outcomes

The preoperative and postoperative delta scores of AAE, ALE, ER, and IR values were significantly different in both groups ($p < .0001$). WOOS index score changed significantly, increasing by a median of .0.47 and 0.51 points in the BIO-RSA and MIO-RSA group, respectively (all $p < 0.001$) (Table 2). No significant correlation was found between fatty infiltration of the teres minor and ER gain. Delta scores of AAE were higher in the MIO-RSA group ($p= 0.027$). The differences in the other planes of shoulder motion and in WOOS index scores between the groups were not significant. Glenosphere

eccentricity and size (36, 39 and 42 mm) affected neither the clinical scores nor shoulder mobility in both the groups.

	BIO-RSA		MIO-RSA		P value (Mann-Whitney test)
Variable	Median (IQR)	Mean (SD)	Median (IQR)	Mean (SD)	
AAE delta score	70 (50-80)	66 (27.7)	87.5 (55-105)	82 (31.3)	*0.027*
ALE delta score	60 (50-80)	61 (26.4)	72 (45-100)	72 (38.5)	0.206
ER delta score	30 (20-50)	34.5 (21.8)	35 (25-65)	41.7 (22.4)	0.291
IR delta score	4 (2-4)	3.1 (3)	2 (2-4)	2.7 (2)	0.590
WOOS index delta score	0.47 (0.04-0.55)	0.46 (0.13)	0.51 (0.36-0.59)	0.48 (0.14)	0.055

Table 2. Active shoulder mobility and clinical scores in BIO-RSA and MIO-RSA group

IQR interquartile range (25th–75th percentile), SD standard deviation, AAE active anterior elevation, ALE active lateral elevation ER external rotation, IR internal rotation, WOOS Western Ontario Osteoarthritis of the Shoulder Index.

AAE, and ER are reported in degrees.

IR is reported as points: 0 = dorsum of hand to lateral thigh to 10 = dorsum of hand to interscapular region. Subscripts 1 and 2 indicate preoperative and postoperative values, respectively

Delta scores: difference between preoperative and postoperative values. The delta scores of the two groups were analyzed with the Mann-Whitney test

Significant values are in italic.

4.3 Postoperative radiographic outcomes

The two groups had a similar rate of glenoid radiolucency, scapular spurs, HO and humerus spot weld. The rate of high position of the glenosphere was higher in the BIO-RSA group ($p = 0.022$). The value of **β** angle was similar in the two groups, with a median of 87.7 degree in the BIO-RSA and 87.5 in the MIO-RSA group. We recorded a similar rate of postoperative glenoid retroversion in the two groups (median: 8 degree).

The correction of B2 type glenoid deformity using a metallic full wedge (15°) baseplate is described in Figure 19 (A-D).

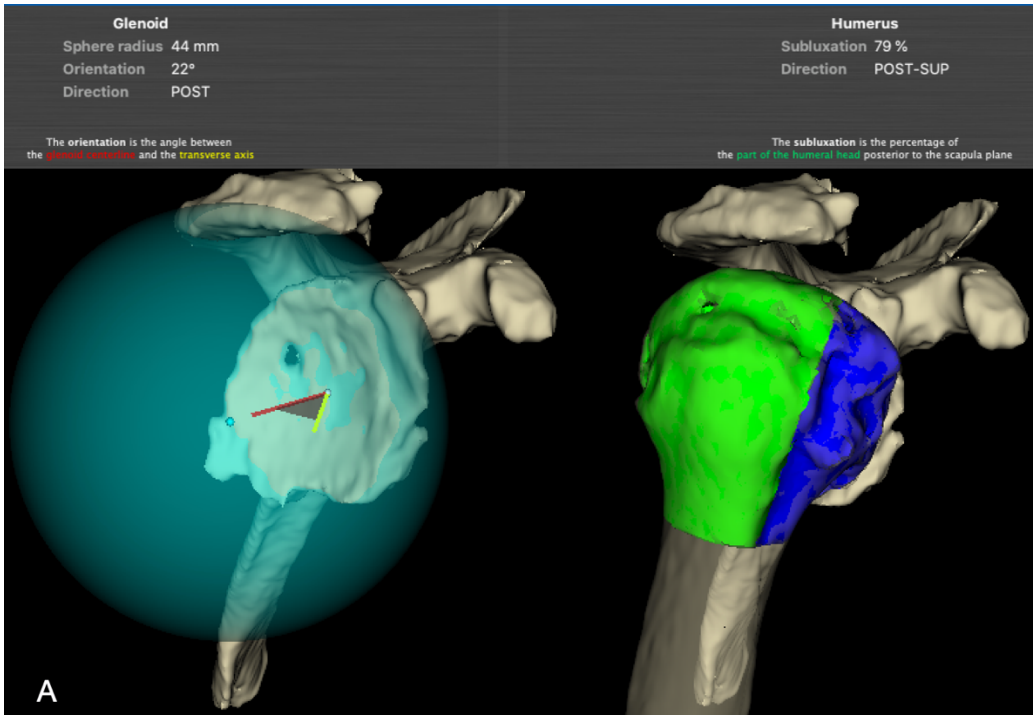
Glenoid
Sphere radius 44 mm
Orientation 22°
Direction POST
Humerus
Subluxation 79 %
Direction POST-SUP
The orientation is the angle between the glenoid centerline and the transverse axis
The subluxation is the percentage of the part of the humeral head posterior to the scapula plane
A

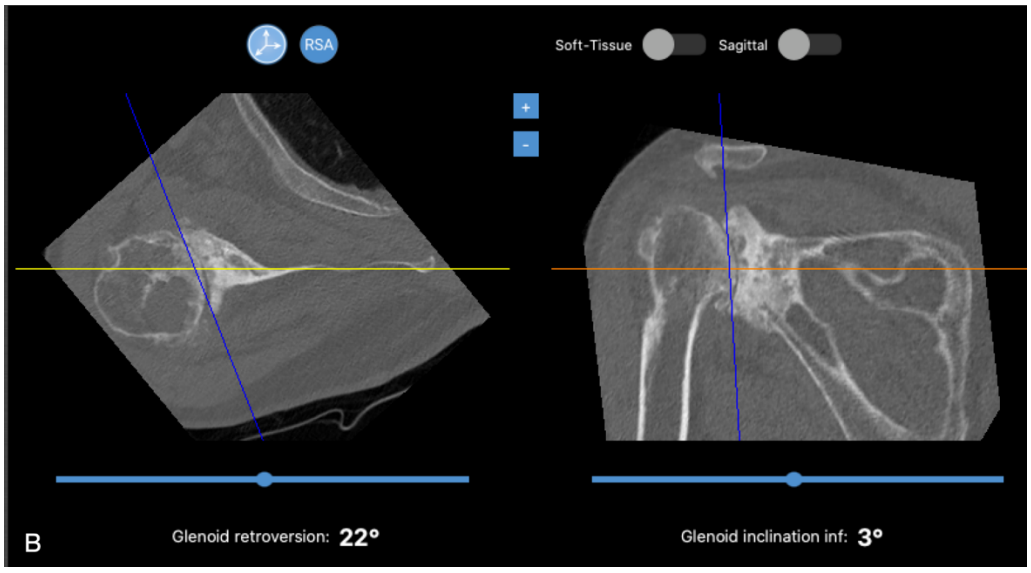
RSA
Soft-Tissue
Sagittal
B
Glenoid retroversion: 22°
Glenoid inclination inf: 3°

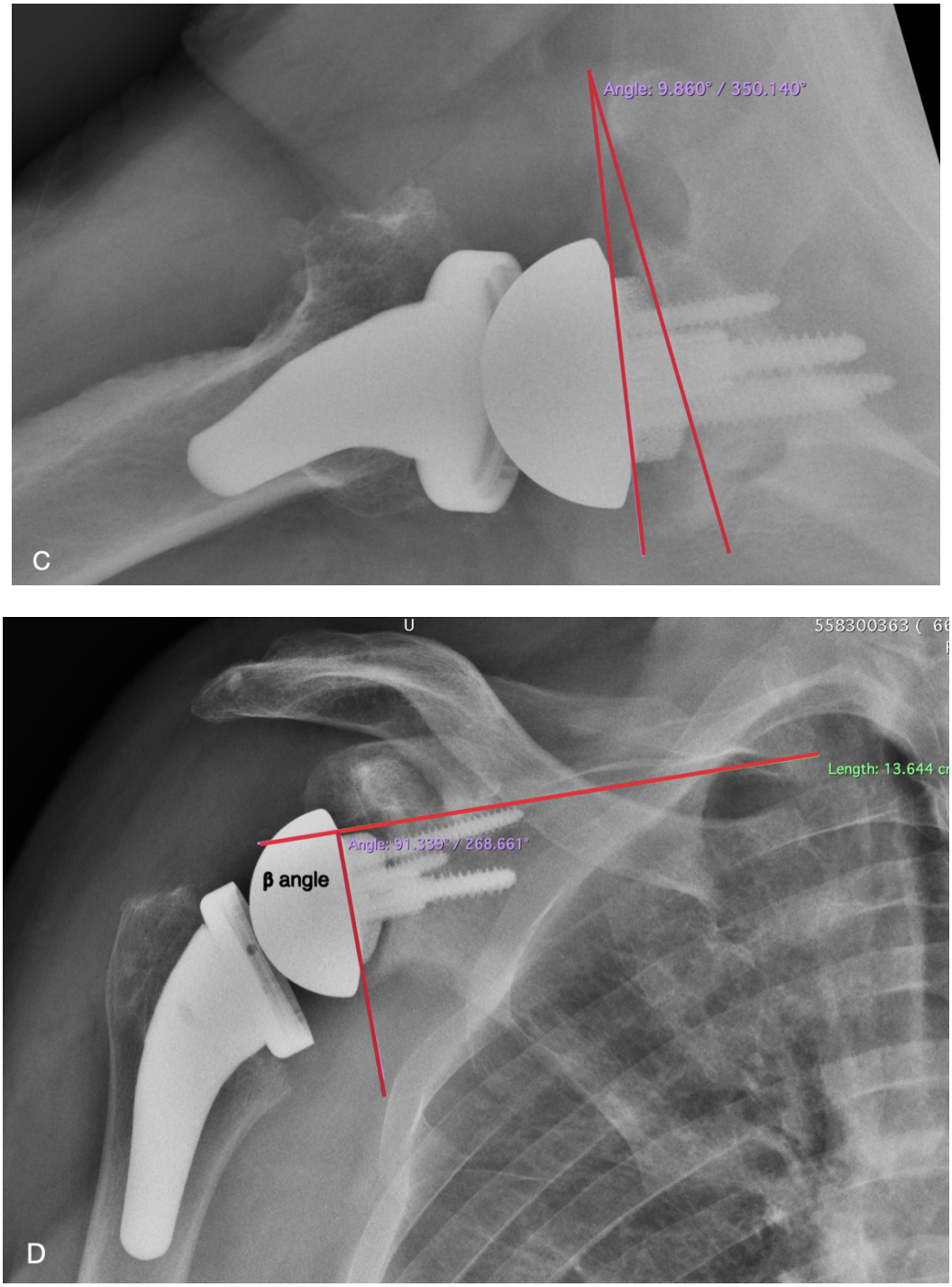

Figure 19. Primary shoulder osteoarthritis with severe glenoid bone loss (B2 glenoid), A) Advanced measures of 3D CT planning representing the orientation (22°) and direction (posterior or posterior-central) of the glenoid wear, and the amount of posterior humeral head subluxation (79%, posterior-superior), B) 2D CT scan with the calculated values of glenoid retroversion and inclination, C)

Postoperative axillary view radiograph after RSA with full-wedge augmented baseplate (15°, 25 mm size) shows improvement of glenoid retroversion with posterior glenoid bone preserving, D) Postoperative true AP view radiograph of the RSA described in the figure 2C with the value of **β** angle explaining the appropriate baseplate inclination.

An eccentric posterior-superior type E3 glenoid wear corrected with angled BIO-RSA is represented in Figure 20 (A-D).

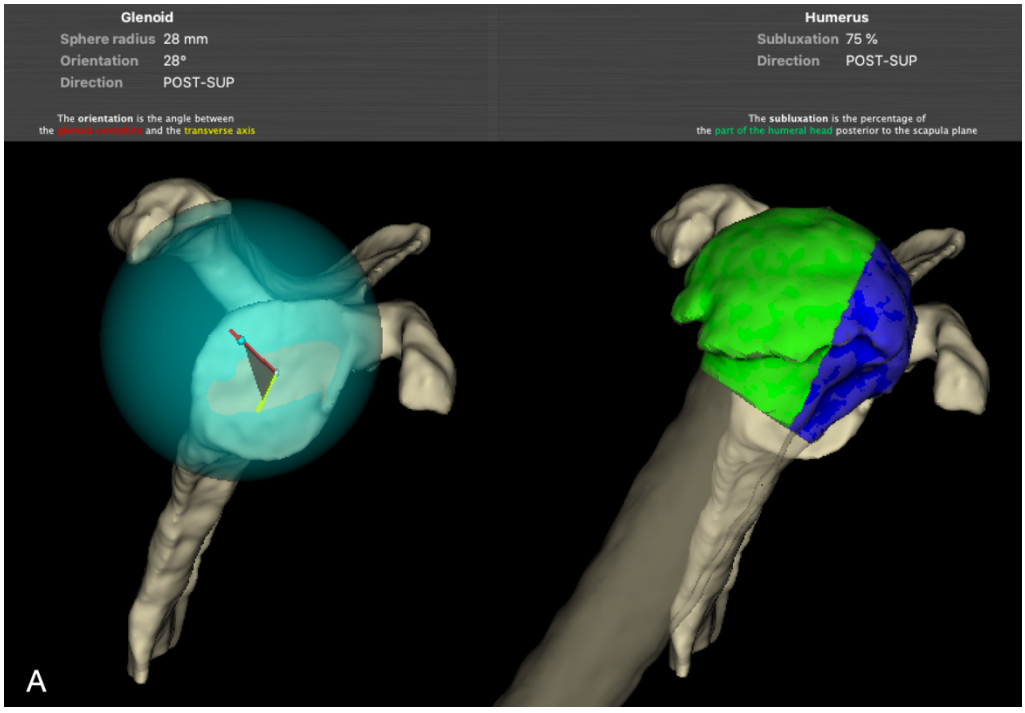
Glenoid
Sphere radius 28 mm
Orientation 28°
Direction POST-SUP
The orientation is the angle between the glenoid centerline and the transverse axis
Humerus
Subluxation 75 %
Direction POST-SUP
The subluxation is the percentage of the part of the humeral head posterior to the scapula plane
A

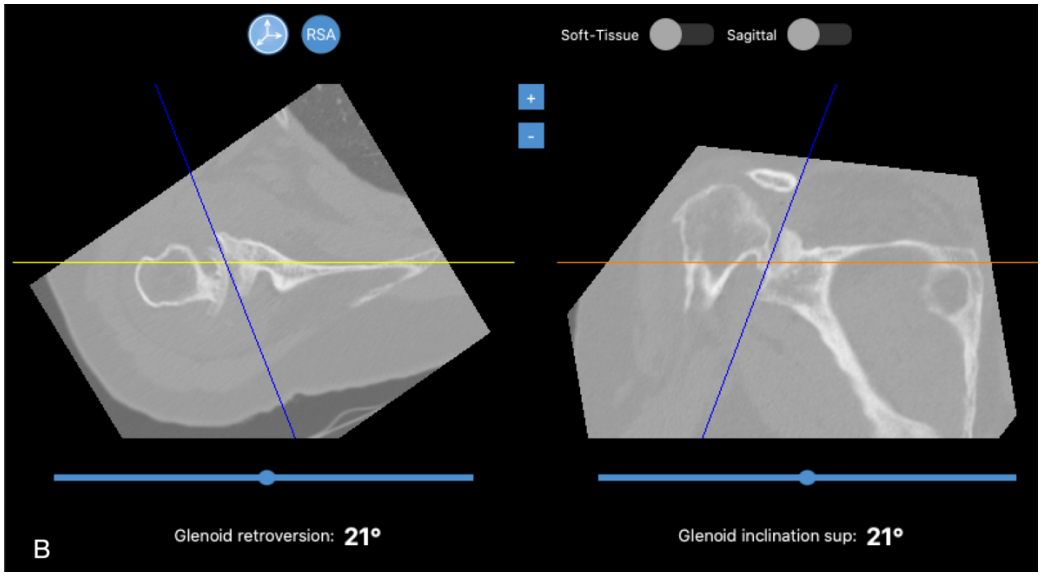
RSA
Soft-Tissue
Sagittal
+
-
B
Glenoid retroversion: 21°
Glenoid inclination sup: 21°

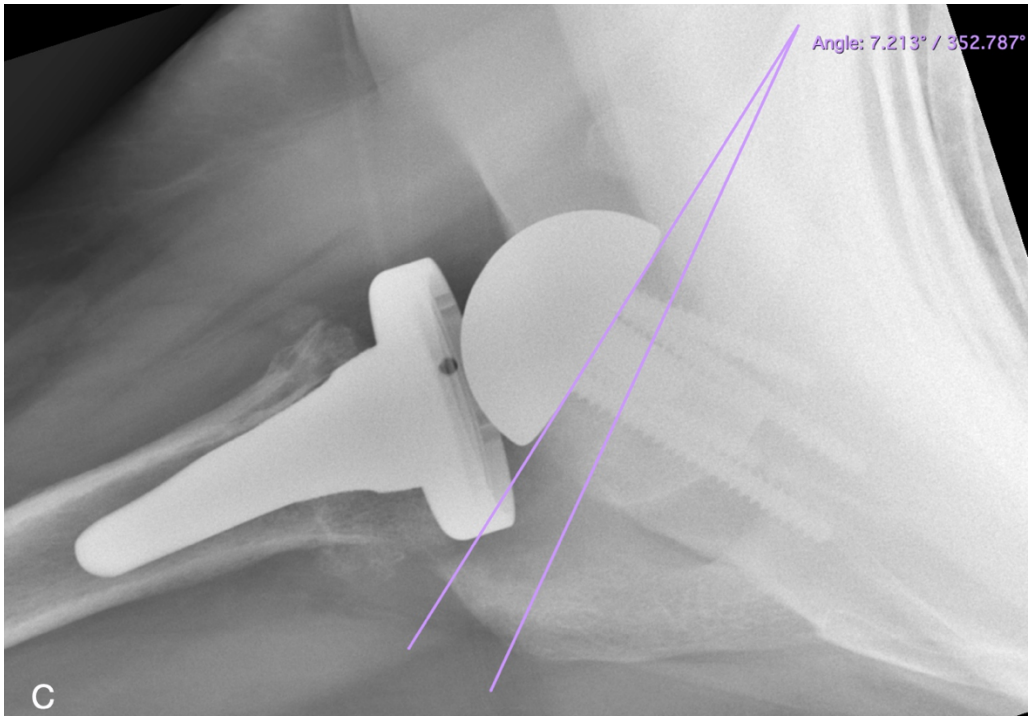
Angle: 7.213° / 352.787°
C

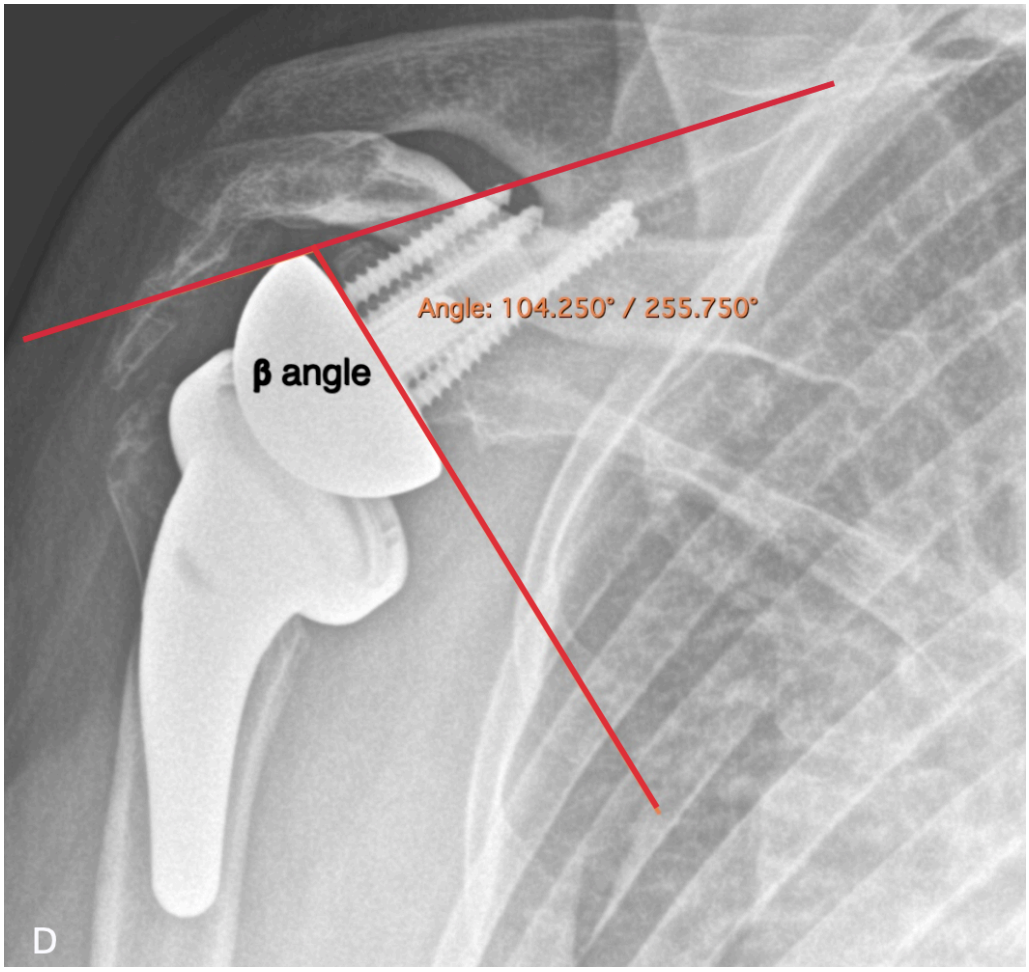
Angle: 104.250° / 255.750°
β angle
D

Figure 20. Cuff tear arthropathy with severe eccentric glenoid wear (E3 glenoid), A) orientation (28°) and direction (posterior-superior) of the glenoid wear, and the amount of posterior-superior humeral head subluxation (75%). B) 2D CT scan with the calculated values of glenoid retroversion and inclination, C) Postoperative axillary view radiograph after BIO-RSA with improvement of glenoid retroversion and good bone graft healing, D) Postoeprative true AP radiograph of the BIO-RSA described in the figure 3C with the value of the **β** angle explaining the appropriate correction of superior glenoid inclination.

Scapular notching was found in 6 patients of BIO-RSA group (grade 1 in four patients and grade 2 in two) and in 1 patient of MIO-RSA group (grade 1), but the difference was not significant. Radiolucent lines < 2mm around bone graft were recorded in the 16 BIO-RSA shoulders (36.4%) and decreased thickness in 15 (34.1%) (Fig. 21)

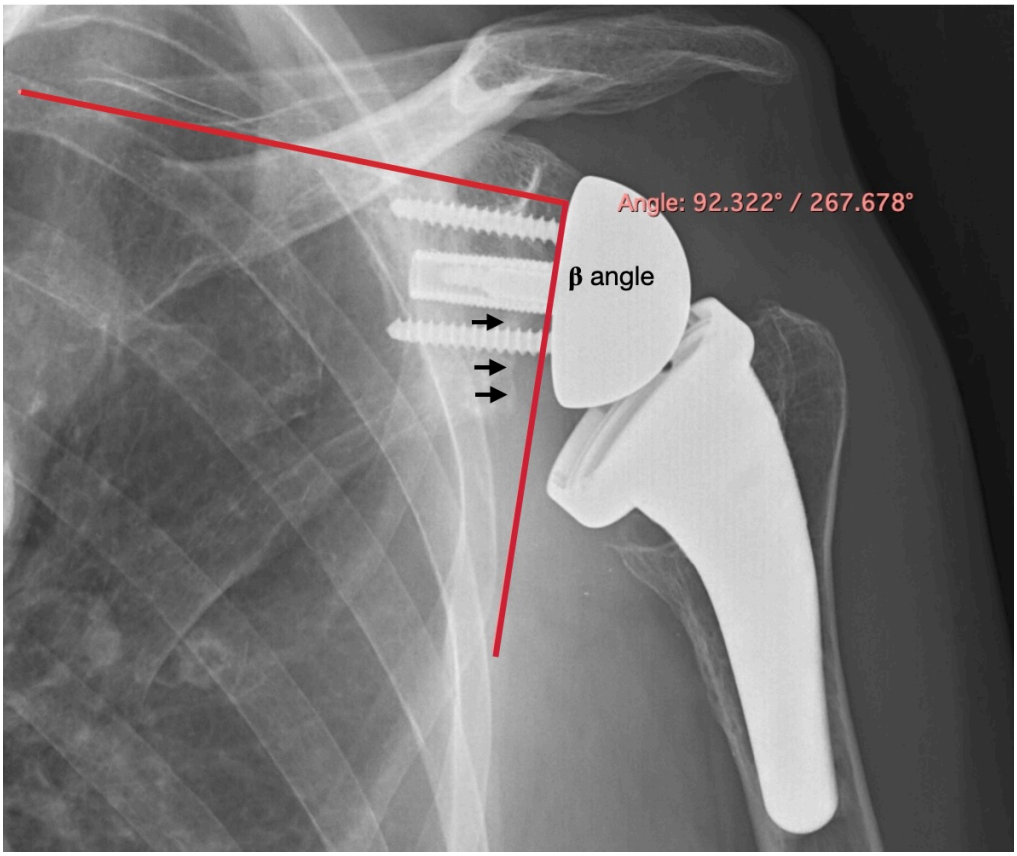

Figure 21. Angled BIO-RSA showing grade II scapular notching and partial resorption of glenoid bone grafting (black arrows).

The overall rate of bone graft healing was 64%. Incomplete baseplate seating (radiolucent lines < 2 mm) were found in 4 MIO-RSA patients (10%). A subgroup analysis showed no effects of preoperative glenoid retroversion and inclination on shoulder mobility and WOOS index. The postoperative X-rays showed a significantly higher rate of humerus condensation lines in MIO-RSA group (p= 0.01) and higher rate of cortical tinning and tuberosity resorption in the BIO-RSA group (p= 0.027 and p = 0.004). A subgroup analysis showed no effects of preoperative glenoid retroversion and inclination on shoulder mobility and WOOS index. Similarly, age, gender and BMI did not affect clinical scores and radiographic outcomes. Radiographic outcomes in the two groups are reported in Table 3.

Variable (n°) (%)	BIO-RSA	MIO-RSA	*P value*
Humeral radiolucent lines			.332
No	38 (86)	34 (87)	
< 2mm	6 (14)	5 (12)	
Humeral condensation lines	4 (9)	16 (40)	*.001*
Humeral cortical thinning	20 (45)	8 (20)	.027
Humeral spot weld	0	3 (7)	.062
Humeral osteolysis	3 (7)	5 (13)	.248
Tuberosity resorption			*.004*
No	27 (61)	37 (95)	
Greater tuberosity	8 (18)	2 (5)	
Lesser tuberosity	7 (16)	0	
Both	2 (5)	0	
Glenoid radiolucent lines			
No	30 (70)	35 (90)	
< 2 mm	14 (30)	4 (10)	
> 2 mm	0	0	
Glenoid scapular notching			.371
Grade 0	38(86)	38(97)	
Grade 1	4 (9)	1 (3)	
Grade 2	2 (4)	0	
Scapular spur	6 (14)	0	.049
Heterotopic Ossifications	2 (5)	0	.889
Glenoid bone graft healing (radiolucent lines)		NA	
No	28 (64)		
< 2 mm	16 (36)		
Bone graft viability (osteolysis/decreased thickness)	15 (34)	NA	
Glenosphere position			
High	5 (11)	1 (3)	
Flush	12 (27)	16 (40)	
Low	26 (59)	15 (39)	
Very low	1 (2)	7 (17)	

Table 3. Radiographic findings in BIO-RSA and MIO-RSA patients

BIO-RSA: bony-increased offset reverse shoulder arthroplasty

MIO-RSA: metallic-increased offset reverse shoulder arthroplasty

Significant values are in italic.

CHAPTER 5

Discussion

Popularity of glenoid augments has increased despite the BIO-RSA being a viable solution to address severe glenoid bone loss[93,160]. Our study compared metal augmented baseplate with BIO-RSA using the same onaly curved-stem and glenosphere, and found that, despite the BIO-RSA cohort having greater preoperative glenoid retroversion, both group achieved significantly higher postoperative shoulder function scores.

The rate of scapular notching was higher in the BIO-RSA group, but the difference was not significant compared with MIO-RSA patients.

Our findings are consistent with Van de Kleut et al who reported only three cases of notching (2 in MIO-RSA patients and one in BIO-RSA) using the same design of lateralized RSA[147]. Colasanti et al, instead, reported higher rate of notching in glenoid bone graft group compared with augmented baseplate, using a different design of glenoid component[161].

Boileau et al[93] observed 25% rate of scapular notching (grade 1 to 3) in their series of BIO-RSA with Grammont style humeral component, and they emphasized that all cases of notching were found with smaller glenosphere (36 mm) and large baseplate (29 mm). The same authors suggested that a minimum of 5 mm of inferior overhang, as well as the use of 25 mm baseplate, would be helpful to reduce the risk of notching. In our series of BIO-RSA we used the same large baseplate as described by Boileau, with an eccentric glenosphere in less than 50% of patients. We believe that our choice of a humeral component with a 145° NSA (132.5° stem inclination combined with and asymmetric 12.5 polyethylene insert) and onlay humeral tray, have substantially contributed to reduce the risk of notching. These findings are in line with our previous research study[132].

High position of the glenosphere was found to be more common in the BIO-RSA patients, that may theoretically explain the higher values of AAE recorded in the MIO-RSA patients. Overall, the value

of postoperative **β** angle found in the two groups demonstrated the reasonable correction of glenoid inclination obtained with bone and metal augmentation, as reported by other authors[93,162].

Boileau et al showed showed a satisfactory correction of posterior and superior glenoid deficiencies using angled BIO-RSA technique, with a mean change of 16° of inclination and 12.8° of retroversion[93].

Kirsch et al reported a mean improvement of 10° of global glenoid inclination as measured by the beta angle in a cohort of patients with B2, B3, E2 and E3 glenoids[162].

Recent studies assessing glenoid erosion in type B2 glenoid found that the majority of glenoid wear had a posterior-inferior[91] or posterior-central[96] direction.

Despite the differences described in the direction of glenoid wear, observations of these studies outlined that the wear in B2 glenoids involve most of the joint surface in posterior, superior and inferior direction.

Abdic et al[148], showed that the orientation of Favard type E2 glenoid erosion was towards the 10:30 clock-face position in the posterior-superior glenoid quadrant. Our preoperative CT measurements are in line with the observations of Otto et al[96] and Abdic et al[148].

The radiographic difference of our study, between the postoperative values of retroversion were not compared with preoperative CT software measurements of glenoid version to avoid bias in quantitative data analysis.

However, the improved values of postoperative glenoid inclination and version, recorded with postoperative standard radiographs, support the need of bony or metallic augmentation to address glenoid deformity and restore reasonable values of glenoid retroversion, close enough to the premorbid glenoid version (range: -7° + 10°)[163].

The excellent seating of the metal augmented baseplate found in axillary radiograph, satisfied both the goals, to fill the bone defect, and to prevent the medialization of the joint line, as demonstrated by Zhou et al[164].

Interestingly, the use of large full-wedge augmented baseplate (29 mm) did not affect final clinical scores, nor produced significant radiological changes around the glenoid component. Metal augmented baseplate corrected the retroversion, restoring a joint line close enough to the values recorded with the simulation of preoperative software planning. Even the length of the screws, size of the glenosphere and humeral components were similar.

Our study showed union between the cancellous bone graft and the surface of the native glenoid in less than 70% of BIO-RSA patients. Two recent research articles described a rate of 23% and 25% of humeral head bone graft resorption in primary RSA, at a mean of 2.8 and 2.6 years, respectively[145,149.] Radiographic signs of graft resorption were associated with radiographic baseplate failures[145]. These findings are not in accordance with those of Boileau et al[93], who reported complete graft incorporation in 94% of patients assessed by CT scan. Although, using standard radiographs to assess bone graft healing and incorporation may represent a limitation of our study, the effectiveness of CT for the detection of bone graft resorption in RSA is controversial[165]. Ferreira et al demonstrated that the sensitivity of CT is inconsistent at visualizing the presence or absence of bone graft resorption adjacent to a RSA glenoid baseplate[165]. Additional studies described 94% to 100% humeral head autograft incorporation in primary RSA using conventional radiographs[166 167]. We may suppose that the difference in age, BMI and percentage of females found in patients of the BIO-RSA group, may have affected the quality of bone graft and related radiographic outcomes. However, data arised from this study seems not to support these speculations. Bone graft healing and viability in BIO-RSA still remains debatable.

We found higher rate of radiological bone adaptations (cortical thinning and tuberosity resorption) around the humeral component of BIO-RSA patients that cannot be explained with the available data of the current study. Several variables could affect these radiographic findings, such as the quality of trabecular bone, the cortical thickness, and intra-operative reaming. The stem-related stress shielding

effect was irrelevant, as the size was similar in the two groups. Despite these radiographic changes, humeral components were stable in both the groups, without significant radiolucent lines or subsidence. Studies comparing clinical and radiographic outcomes of BIO-RSA and metal augmented baseplate RSA are lacking. Two studies performed a comparative analysis of the same implant design assessed in our study. A randomized clinical trial by Van de Kleut et al[147] compared glenoid implant migration between BIO-RSA and metal augmented baseplate, using model-based radiostereometric analysis. At two year follow-up their results indicated both implants provided stable fixation without substantial difference in clinical outcomes. Despite the high level of evidence, this study include a smaller sample size than that required with a power of 0.8 at two year follow-up (35 patients), also stated by the authors in the limitations of their study. They also found a limited improvement in external rotation in the metal augment cohort, that was ascribed to the single geometry (15°) of the metal augment, compared to the bone graft of BIO-RSA cohort that was shaped to address specific glenoid defects. These findings are not in line with our study, as the values of external rotation were similar in both the groups. We think that the large cohort of patients included in our study has provided more reliable data that explain the differences on the values of external rotation.

Nabergoj et al[146], retrospectively compared clinical and radiographic outcomes of RSA with combined bony and metallic augment (BMA), and bony augmentation (BA) alone in 16 patients (8 per group). The BMA group had significantly different glenoid morphology and greater bone loss thickness than the BA group. They found higher improvement of forward flexion and Constant score in BMA group and higher external rotation in BA group. Even for this study the same consideration of sample size apply in order to be reliable.

A retrospective study of Colasanti et al[161] compared BIO-RSA (39 patients) with augmented glenoid baseplate RSA (442 patients), using a reverse design different from that used in our study. At a mean 2 years follow-up, the augmented baseplate group showed better clinical scores and lower rate of

scapular notching and adverse radiographic findings. The marked difference of the sample size in the two groups raise doubt in the analysis of their data. The augmented glenoid patients showed higher improvement of forward flexion and similar external rotation values, in line with the results of our study. Furthermore, the baseplate described by Colasanti et al, as outlined above, has three different design of the metallic augment (posterior, superior and combined), and of variable degree (8° to 10°). As such, the similarities with clinical metrics of our study should be interpreted with caution and not overstated. The present study has four major limitations: i) the retrospective design, ii) the medium-term follow-up, which prevents drawing definitive conclusions on the risk of bone graft resorption and implant survival in BIO-RSA patients; iii) the use of conventional radiographs to assess postoperative glenoid version and inclination that preclude a comparison with preoperative CT data; iv) higher BMI, age and percentage of females in BIO-RSA patients may have affected the quality of glenoid bone graft and related radiological changes over time.

5.1 Conclusion

Metal augment is a viable alternative to BIO-RSA to preserve bone and prevent the medialization of joint line in arthritic glenoids with multiplanar deformity. The mid-term outcomes of the two implants show that the bone graft and metallic glenoid augmentation, both provide good clinical outcomes. The not negligible rate of bone graft resorption in BIO-RSA patient raise concern about the risk of scapular notching and baseplate loosening in the long-term.

References

1. Bakhsh W, Nicandri G. Anatomy and Physical Examination of the Shoulder. *Sports Med Arthrosc Rev*. Sep 2018;26(3):e10-e22. doi:10.1097/JSA.0000000000000202
2. Moore K DA. Clinically Oriented Anatomy, 4th ed. . *New York, NY: Lippincott Williams & Wilkins*. 1999;
3. Moore KL DA, Agur AMR. Upper Extremity Clinically Oriented Anatomy. *Wolters Kluwer Health/Lippincott Williams & Wilkins;*. 2014;
4. Terry GC, Chopp TM. Functional anatomy of the shoulder. *J Athl Train*. Jul 2000;35(3):248-55.
5. Howell SM, Galinat BJ. The glenoid-labral socket. A constrained articular surface. *Clin Orthop Relat Res*. Jun 1989;(243):122-5.
6. Ide J, Maeda S, Takagi K. Normal variations of the glenohumeral ligament complex: an anatomic study for arthroscopic Bankart repair. *Arthroscopy*. Feb 2004;20(2):164-8. doi:10.1016/j.arthro.2003.11.005
7. Boardman ND, Debski RE, Warner JJ, et al. Tensile properties of the superior glenohumeral and coracohumeral ligaments. *J Shoulder Elbow Surg*. Jul-Aug 1996;5(4):249-54. doi:10.1016/s1058-2746(96)80050-4
8. Fox AJS, Fox OJK, Schar MO, Chaudhury S, Warren RF, Rodeo SA. The glenohumeral ligaments: Superior, middle, and inferior: Anatomy, biomechanics, injury, and diagnosis. *Clin Anat*. Mar 2021;34(2):283-296. doi:10.1002/ca.23717
9. Ticker JB, Flatow EL, Pawluk RJ, et al. The inferior glenohumeral ligament: a correlative investigation. *J Shoulder Elbow Surg*. Nov-Dec 2006;15(6):665-74. doi:10.1016/j.jse.2005.11.006
10. Ticker JB, Bigliani LU, Soslowsky LJ, Pawluk RJ, Flatow EL, Mow VC. Inferior glenohumeral ligament: geometric and strain-rate dependent properties. *J Shoulder Elbow Surg*. Jul-Aug 1996;5(4):269-79. doi:10.1016/s1058-2746(96)80053-x
11. McCausland C, Sawyer E, Eovaldi BJ, Varacallo M. Anatomy, Shoulder and Upper Limb, Shoulder Muscles. *StatPearls*. 2022.
12. Merolla G, Paladini P, Artiaco S, Tos P, Lollino N, Porcellini G. Surgical repair of acute and chronic pectoralis major tendon rupture: clinical and ultrasound outcomes at a mean follow-up of 5 years. *Eur J Orthop Surg Traumatol*. Jan 2015;25(1):91-8. doi:10.1007/s00590-014-1451-y
13. Merolla G, Campi F, Paladini P, Porcellini G. Surgical approach to acute pectoralis major tendon rupture. *G Chir*. Jan-Feb 2009;30(1-2):53-7.
14. Merolla G, Paladini P, Campi F, Porcellini G. Pectoralis major tendon rupture. Surgical procedures review. *Muscles Ligaments Tendons J*. Apr 2012;2(2):96-103.
15. Maruvada S, Madrazo-Ibarra A, Varacallo M. Anatomy, Rotator Cuff. *StatPearls*. 2022.
16. DeFranco MJ, Cole BJ. Current perspectives on rotator cuff anatomy. *Arthroscopy*. Mar 2009;25(3):305-20. doi:10.1016/j.arthro.2008.07.023
17. Gupta H, Robinson P. Normal shoulder ultrasound: anatomy and technique. *Semin Musculoskelet Radiol*. Jul 2015;19(3):203-11. doi:10.1055/s-0035-1549315
18. Bailie DS, Moseley B, Lowe WR. Surgical anatomy of the posterior shoulder: effects of arm position and anterior-inferior capsular shift. *J Shoulder Elbow Surg*. Jul-Aug 1999;8(4):307-13. doi:10.1016/s1058-2746(99)90151-9
19. Burkhead WZ, Jr., Scheinberg RR, Box G. Surgical anatomy of the axillary nerve. *J Shoulder Elbow Surg*. Jan 1992;1(1):31-6. doi:10.1016/S1058-2746(09)80014-1

20. Uz A, Apaydin N, Bozkurt M, Elhan A. The anatomic branch pattern of the axillary nerve. *J Shoulder Elbow Surg*. Mar-Apr 2007;16(2):240-4. doi:10.1016/j.jse.2006.05.003
21. Flatow EL, Bigliani LU, April EW. An anatomic study of the musculocutaneous nerve and its relationship to the coracoid process. *Clin Orthop Relat Res*. Jul 1989;(244):166-71.
22. Yang HJ, Gil YC, Jin JD, Ahn SV, Lee HY. Topographical anatomy of the suprascapular nerve and vessels at the suprascapular notch. *Clin Anat*. Apr 2012;25(3):359-65. doi:10.1002/ca.21248
23. Jobe CM PWaPD. Gross Anatomy of the Shoulder. *in Rockwood and Matsen ed: The Shoulder 5th edition Elsevier Science 2017*. 2016;(Chapter 2):35-94.
24. Cooper DE, O'Brien SJ, Warren RF. Supporting layers of the glenohumeral joint. An anatomic study. *Clin Orthop Relat Res*. Apr 1993;(289):144-55.
25. Harkness EF, Macfarlane GJ, Silman AJ, McBeth J. Is musculoskeletal pain more common now than 40 years ago?: Two population-based cross-sectional studies. *Rheumatology (Oxford)*. Jul 2005;44(7):890-5. doi:10.1093/rheumatology/keh599
26. Cadogan A, Laslett M, Hing WA, McNair PJ, Coates MH. A prospective study of shoulder pain in primary care: prevalence of imaged pathology and response to guided diagnostic blocks. *BMC Musculoskelet Disord*. May 28 2011;12:119. doi:10.1186/1471-2474-12-119
27. Cho HJ, Morey V, Kang JY, Kim KW, Kim TK. Prevalence and Risk Factors of Spine, Shoulder, Hand, Hip, and Knee Osteoarthritis in Community-dwelling Koreans Older Than Age 65 Years. *Clin Orthop Relat Res*. Oct 2015;473(10):3307-14. doi:10.1007/s11999-015-4450-3
28. Oh JH, Chung SW, Oh CH, et al. The prevalence of shoulder osteoarthritis in the elderly Korean population: association with risk factors and function. *J Shoulder Elbow Surg*. Jul 2011;20(5):756-63. doi:10.1016/j.jse.2011.01.021
29. Kobayashi T, Takagishi K, Shitara H, et al. Prevalence of and risk factors for shoulder osteoarthritis in Japanese middle-aged and elderly populations. *J Shoulder Elbow Surg*. May 2014;23(5):613-9. doi:10.1016/j.jse.2013.11.031
30. Saltzman MD, Mercer DM, Warme WJ, Bertelsen AL, Matsen FA, 3rd. Comparison of patients undergoing primary shoulder arthroplasty before and after the age of fifty. *J Bone Joint Surg Am*. Jan 2010;92(1):42-7. doi:10.2106/JBJS.I.00071
31. Ibounig T, Simons T, Launonen A, Paavola M. Glenohumeral osteoarthritis: an overview of etiology and diagnostics. *Scand J Surg*. Sep 2021;110(3):441-451. doi:10.1177/1457496920935018
32. Kerr R, Resnick D, Pineda C, Haghighi P. Osteoarthritis of the glenohumeral joint: a radiologic-pathologic study. *AJR Am J Roentgenol*. May 1985;144(5):967-72. doi:10.2214/ajr.144.5.967
33. Neer CS, 2nd. Replacement arthroplasty for glenohumeral osteoarthritis. *J Bone Joint Surg Am*. Jan 1974;56(1):1-13.
34. Dieppe PA, Lohmander LS. Pathogenesis and management of pain in osteoarthritis. *Lancet*. Mar 12-18 2005;365(9463):965-73. doi:10.1016/S0140-6736(05)71086-2
35. Zhang Y, Jordan JM. Epidemiology of osteoarthritis. *Clin Geriatr Med*. Aug 2010;26(3):355-69. doi:10.1016/j.cger.2010.03.001
36. Doherty M, Watt I, Dieppe P. Influence of primary generalised osteoarthritis on development of secondary osteoarthritis. *Lancet*. Jul 2 1983;2(8340):8-11. doi:10.1016/s0140-6736(83)90003-x
37. Fernandez-Moreno M, Rego I, Carreira-Garcia V, Blanco FJ. Genetics in osteoarthritis. *Curr Genomics*. Dec 2008;9(8):542-7. doi:10.2174/138920208786847953
38. Loughlin J. Genetic contribution to osteoarthritis development: current state of evidence. *Curr Opin Rheumatol*. May 2015;27(3):284-8. doi:10.1097/BOR.0000000000000171

39. Chapman K, Valdes AM. Genetic factors in OA pathogenesis. *Bone*. Aug 2012;51(2):258-64. doi:10.1016/j.bone.2011.11.026
40. Silverwood V, Blagojevic-Bucknall M, Jinks C, Jordan JL, Protheroe J, Jordan KP. Current evidence on risk factors for knee osteoarthritis in older adults: a systematic review and meta-analysis. *Osteoarthritis Cartilage*. Apr 2015;23(4):507-15. doi:10.1016/j.joca.2014.11.019
41. Thijssen E, van Caam A, van der Kraan PM. Obesity and osteoarthritis, more than just wear and tear: pivotal roles for inflamed adipose tissue and dyslipidaemia in obesity-induced osteoarthritis. *Rheumatology (Oxford)*. Apr 2015;54(4):588-600. doi:10.1093/rheumatology/keu464
42. Tu C, He J, Wu B, Wang W, Li Z. An extensive review regarding the adipokines in the pathogenesis and progression of osteoarthritis. *Cytokine*. Jan 2019;113:1-12. doi:10.1016/j.cyto.2018.06.019
43. Sanchez-Adams J, Leddy HA, McNulty AL, O'Conor CJ, Guilak F. The mechanobiology of articular cartilage: bearing the burden of osteoarthritis. *Curr Rheumatol Rep*. Oct 2014;16(10):451. doi:10.1007/s11926-014-0451-6
44. Gurer G, Bozbas GT, Tuncer T, Unubol AI, Ucar UG, Memetoglu OI. Frequency of joint hypermobility in Turkish patients with knee osteoarthritis: a cross sectional multicenter study. *Int J Rheum Dis*. Oct 2018;21(10):1787-1792. doi:10.1111/1756-185X.12883
45. Sharma L, Dunlop DD, Cahue S, Song J, Hayes KW. Quadriceps strength and osteoarthritis progression in malaligned and lax knees. *Ann Intern Med*. Apr 15 2003;138(8):613-9. doi:10.7326/0003-4819-138-8-200304150-00006
46. Millett PJ, Gobezie R, Boykin RE. Shoulder osteoarthritis: diagnosis and management. *Am Fam Physician*. Sep 1 2008;78(5):605-11.
47. Maquirriain J, Ghisi JP, Amato S. Is tennis a predisposing factor for degenerative shoulder disease? A controlled study in former elite players. *Br J Sports Med*. May 2006;40(5):447-50. doi:10.1136/bjsm.2005.023382
48. Carfagno DG, Ellenbecker TS. Osteoarthritis of the glenohumeral joint: nonsurgical treatment options. *Phys Sportsmed*. Apr 2002;30(4):19-30. doi:10.3810/psm.2002.04.253
49. Moor BK, Bouaicha S, Rothenfluh DA, Sukthankar A, Gerber C. Is there an association between the individual anatomy of the scapula and the development of rotator cuff tears or osteoarthritis of the glenohumeral joint?: A radiological study of the critical shoulder angle. *Bone Joint J*. Jul 2013;95-B(7):935-41. doi:10.1302/0301-620X.95B7.31028
50. Allen B, Schoch B, Sperling JW, Cofield RH. Shoulder arthroplasty for osteoarthritis secondary to glenoid dysplasia: an update. *J Shoulder Elbow Surg*. Feb 2014;23(2):214-20. doi:10.1016/j.jse.2013.05.012
51. Johnson MH, Paxton ES, Green A. Shoulder arthroplasty options in young (<50 years old) patients: review of current concepts. *J Shoulder Elbow Surg*. Feb 2015;24(2):317-25. doi:10.1016/j.jse.2014.09.029
52. Harper KW, Helms CA, Haystead CM, Higgins LD. Glenoid dysplasia: incidence and association with posterior labral tears as evaluated on MRI. *AJR Am J Roentgenol*. Mar 2005;184(3):984-8. doi:10.2214/ajr.184.3.01840984
53. Kambhampati SB, Birch R, Cobiella C, Chen L. Posterior subluxation and dislocation of the shoulder in obstetric brachial plexus palsy. *J Bone Joint Surg Br*. Feb 2006;88(2):213-9. doi:10.1302/0301-620X.88B2.17185
54. Pearl ML, Edgerton BW, Kon DS, et al. Comparison of arthroscopic findings with magnetic resonance imaging and arthrography in children with glenohumeral deformities secondary to brachial

plexus birth palsy. *J Bone Joint Surg Am*. May 2003;85(5):890-8. doi:10.2106/00004623-200305000-00018
55. Waters PM, Smith GR, Jaramillo D. Glenohumeral deformity secondary to brachial plexus birth palsy. *J Bone Joint Surg Am*. May 1998;80(5):668-77. doi:10.2106/00004623-199805000-00007
56. Olofsson PN, Chu A, McGrath AM. The Pathogenesis of Glenohumeral Deformity and Contracture Formation in Obstetric Brachial Plexus Palsy-A Review. *J Brachial Plex Peripher Nerve Inj*. Jan 2019;14(1):e24-e34. doi:10.1055/s-0039-1692420
57. Kavaja L, Pajarinen J, Sinisaari I, et al. Arthrosis of glenohumeral joint after arthroscopic Bankart repair: a long-term follow-up of 13 years. *J Shoulder Elbow Surg*. Mar 2012;21(3):350-5. doi:10.1016/j.jse.2011.04.023
58. Hovelius L, Saeboe M. Neer Award 2008: Arthropathy after primary anterior shoulder dislocation--223 shoulders prospectively followed up for twenty-five years. *J Shoulder Elbow Surg*. May-Jun 2009;18(3):339-47. doi:10.1016/j.jse.2008.11.004
59. van der Zwaag HM, Brand R, Obermann WR, Rozing PM. Glenohumeral osteoarthrosis after Putti-Platt repair. *J Shoulder Elbow Surg*. May-Jun 1999;8(3):252-8. doi:10.1016/s1058-2746(99)90138-6
60. Plath JE, Aboalata M, Seppel G, et al. Prevalence of and Risk Factors for Dislocation Arthropathy: Radiological Long-term Outcome of Arthroscopic Bankart Repair in 100 Shoulders at an Average 13-Year Follow-up. *Am J Sports Med*. May 2015;43(5):1084-90. doi:10.1177/0363546515570621
61. Marx RG, McCarty EC, Montemurno TD, Altchek DW, Craig EV, Warren RF. Development of arthrosis following dislocation of the shoulder: a case-control study. *J Shoulder Elbow Surg*. Jan-Feb 2002;11(1):1-5. doi:10.1067/mse.2002.119388
62. Hamada K, Yamanaka K, Uchiyama Y, Mikasa T, Mikasa M. A radiographic classification of massive rotator cuff tear arthritis. *Clin Orthop Relat Res*. Sep 2011;469(9):2452-60. doi:10.1007/s11999-011-1896-9
63. Hamada K, Fukuda H, Mikasa M, Kobayashi Y. Roentgenographic findings in massive rotator cuff tears. A long-term observation. *Clin Orthop Relat Res*. May 1990;(254):92-6.
64. Walch G, Edwards TB, Boulahia A, Nove-Josserand L, Neyton L, Szabo I. Arthroscopic tenotomy of the long head of the biceps in the treatment of rotator cuff tears: clinical and radiographic results of 307 cases. *J Shoulder Elbow Surg*. May-Jun 2005;14(3):238-46. doi:10.1016/j.jse.2004.07.008
65. Dieppe PA, Doherty M, Macfarlane DG, Hutton CW, Bradfield JW, Watt I. Apatite associated destructive arthritis. *Br J Rheumatol*. May 1984;23(2):84-91. doi:10.1093/rheumatology/23.2.84
66. Matsen FA, 3rd, Papadonikolakis A. Published evidence demonstrating the causation of glenohumeral chondrolysis by postoperative infusion of local anesthetic via a pain pump. *J Bone Joint Surg Am*. Jun 19 2013;95(12):1126-34. doi:10.2106/JBJS.L.01104
67. Lehtinen JT, Kaarela K, Belt EA, Kautiainen HJ, Kauppi MJ, Lehto MU. Incidence of glenohumeral joint involvement in seropositive rheumatoid arthritis. A 15 year endpoint study. *J Rheumatol*. Feb 2000;27(2):347-50.
68. Matsen FA III RCJ, Wirth MA. Glenohumeral arthritis and its management. *In: Rockwood CA Jr, Matsen FA III (Eds) The Shoulder Saunders, Philadelphia, PA*. 1998:840-964.
69. Hasan SS, Romeo AA. Nontraumatic osteonecrosis of the humeral head. *J Shoulder Elbow Surg*. May-Jun 2002;11(3):281-98. doi:10.1067/mse.2002.124347
70. Snoddy MC, Lee DH, Kuhn JE. Charcot shoulder and elbow: a review of the literature and update on treatment. *J Shoulder Elbow Surg*. Mar 2017;26(3):544-552. doi:10.1016/j.jse.2016.10.015

71. Friedman RJ, Hawthorne KB, Genez BM. The use of computerized tomography in the measurement of glenoid version. *J Bone Joint Surg Am*. Aug 1992;74(7):1032-7.
72. Habermeyer P, Magosch P, Luz V, Lichtenberg S. Three-dimensional glenoid deformity in patients with osteoarthritis: a radiographic analysis. *J Bone Joint Surg Am*. Jun 2006;88(6):1301-7. doi:10.2106/JBJS.E.00622
73. Bryce CD, Davison AC, Lewis GS, Wang L, Flemming DJ, Armstrong AD. Two-dimensional glenoid version measurements vary with coronal and sagittal scapular rotation. *J Bone Joint Surg Am*. Mar 2010;92(3):692-9. doi:10.2106/JBJS.I.00177
74. Bokor DJ, O'Sullivan MD, Hazan GJ. Variability of measurement of glenoid version on computed tomography scan. *J Shoulder Elbow Surg*. Nov-Dec 1999;8(6):595-8. doi:10.1016/s1058-2746(99)90096-4
75. Verstraeten T, De Wilde L, Victor J. The Normal 3D Gleno-humeral Relationship and Anatomy of the Glenoid Planes. *J Belg Soc Radiol*. Jan 31 2018;102(1):18. doi:10.5334/jbsr.1346
76. Boileau P, Walch G. The three-dimensional geometry of the proximal humerus. Implications for surgical technique and prosthetic design. *J Bone Joint Surg Br*. Sep 1997;79(5):857-65. doi:10.1302/0301-620x.79b5.7579
77. Hertel R, Knothe U, Ballmer FT. Geometry of the proximal humerus and implications for prosthetic design. *J Shoulder Elbow Surg*. Jul-Aug 2002;11(4):331-8. doi:10.1067/mse.2002.124429
78. Amadi HO, Sanghavi SM, Kamineni S, Skourat R, Hansen UN, Bull AM. Definition of the capsular insertion plane on the proximal humerus. *J Anat*. Jun 2008;212(6):863-7. doi:10.1111/j.1469-7580.2008.00903.x
79. Prescher A, Klumpen T. The glenoid notch and its relation to the shape of the glenoid cavity of the scapula. *J Anat*. Apr 1997;190 (Pt 3)(Pt 3):457-60. doi:10.1046/j.1469-7580.1997.19030457.x
80. De Wilde LF BB, Audenaert E, Sys G, Van Maele GO, Barbaix E. About the variability of the shape of the glenoid cavity. *Surg Radiol Anat*. 2004;26(1):54-59. doi:10.1007/s00276-003-0167-1.
81. Huysmans PE, Haen PS, Kidd M, Dhert WJ, Willems JW. The shape of the inferior part of the glenoid: a cadaveric study. *J Shoulder Elbow Surg*. Nov-Dec 2006;15(6):759-63. doi:10.1016/j.jse.2005.09.001
82. Walch G, Badet R, Boulahia A, Khoury A. Morphologic study of the glenoid in primary glenohumeral osteoarthritis. *J Arthroplasty*. Sep 1999;14(6):756-60. doi:10.1016/s0883-5403(99)90232-2
83. Kidder JF RD, DeFranco MJ, Pons-Villanueva J, Dynamidis S. Revisited: Walch classification of the glenoid in glenohumeral
osteoarthritis. *Shoulder Elbow*. 2012;4:11-15. doi::10.1111/j.1758-5740.2011.00151.x
84. Nowak DD, Gardner TR, Bigliani LU, Levine WN, Ahmad CS. Interobserver and intraobserver reliability of the Walch classification in primary glenohumeral arthritis. *J Shoulder Elbow Surg*. Mar 2010;19(2):180-3. doi:10.1016/j.jse.2009.08.003
85. Scalise JJ, Codsi MJ, Brems JJ, Iannotti JP. Inter-rater reliability of an arthritic glenoid morphology classification system. *J Shoulder Elbow Surg*. Jul-Aug 2008;17(4):575-7. doi:10.1016/j.jse.2007.12.006
86. Scalise JJ, Codsi MJ, Bryan J, Brems JJ, Iannotti JP. The influence of three-dimensional computed tomography images of the shoulder in preoperative planning for total shoulder arthroplasty. *J Bone Joint Surg Am*. Nov 2008;90(11):2438-45. doi:10.2106/JBJS.G.01341

87. Budge MD, Lewis GS, Schaefer E, Coquia S, Flemming DJ, Armstrong AD. Comparison of standard two-dimensional and three-dimensional corrected glenoid version measurements. *J Shoulder Elbow Surg*. Jun 2011;20(4):577-83. doi:10.1016/j.jse.2010.11.003
88. Daggett M, Werner B, Gauci MO, Chaoui J, Walch G. Comparison of glenoid inclination angle using different clinical imaging modalities. *J Shoulder Elbow Surg*. Feb 2016;25(2):180-5. doi:10.1016/j.jse.2015.07.001
89. Kwon YW, Powell KA, Yum JK, Brems JJ, Iannotti JP. Use of three-dimensional computed tomography for the analysis of the glenoid anatomy. *J Shoulder Elbow Surg*. Jan-Feb 2005;14(1):85-90. doi:10.1016/j.jse.2004.04.011
90. Bercik MJ, Kruse K, 2nd, Yalizis M, Gauci MO, Chaoui J, Walch G. A modification to the Walch classification of the glenoid in primary glenohumeral osteoarthritis using three-dimensional imaging. *J Shoulder Elbow Surg*. Oct 2016;25(10):1601-6. doi:10.1016/j.jse.2016.03.010
91. Beuckelaers E, Jacxsens M, Van Tongel A, De Wilde LF. Three-dimensional computed tomography scan evaluation of the pattern of erosion in type B glenoids. *J Shoulder Elbow Surg*. Jan 2014;23(1):109-16. doi:10.1016/j.jse.2013.04.009
92. Knowles NK, Keener JD, Ferreira LM, Athwal GS. Quantification of the position, orientation, and surface area of bone loss in type B2 glenoids. *J Shoulder Elbow Surg*. Apr 2015;24(4):503-10. doi:10.1016/j.jse.2014.08.021
93. Boileau P, Morin-Salvo N, Gauci MO, et al. Angled BIO-RSA (bony-increased offset-reverse shoulder arthroplasty): a solution for the management of glenoid bone loss and erosion. *J Shoulder Elbow Surg*. Dec 2017;26(12):2133-2142. doi:10.1016/j.jse.2017.05.024
94. Donohue KW, Ricchetti ET, Iannotti JP. Surgical management of the biconcave (B2) glenoid. *Curr Rev Musculoskelet Med*. Mar 2016;9(1):30-9. doi:10.1007/s12178-016-9315-1
95. Hsu JE, Ricchetti ET, Huffman GR, Iannotti JP, Glaser DL. Addressing glenoid bone deficiency and asymmetric posterior erosion in shoulder arthroplasty. *J Shoulder Elbow Surg*. Sep 2013;22(9):1298-308. doi:10.1016/j.jse.2013.04.014
96. Otto A, Scheiderer B, Murphy M, et al. Biconcave glenoids show 3 differently oriented posterior erosion patterns. *J Shoulder Elbow Surg*. Nov 2021;30(11):2620-2628. doi:10.1016/j.jse.2021.04.028
97. Frankle MA, Teramoto A, Luo ZP, Levy JC, Pupello D. Glenoid morphology in reverse shoulder arthroplasty: classification and surgical implications. *J Shoulder Elbow Surg*. Nov-Dec 2009;18(6):874-85. doi:10.1016/j.jse.2009.02.013
98. Klein SM, Dunning P, Mulieri P, Pupello D, Downes K, Frankle MA. Effects of acquired glenoid bone defects on surgical technique and clinical outcomes in reverse shoulder arthroplasty. *J Bone Joint Surg Am*. May 2010;92(5):1144-54. doi:10.2106/JBJS.I.00778
99. Visotsky JL, Basamania C, Seebauer L, Rockwood CA, Jensen KL. Cuff tear arthropathy: pathogenesis, classification, and algorithm for treatment. *J Bone Joint Surg Am*. 2004;86-A Suppl 2:35-40.
100. Sirveaux F, Favard L, Oudet D, Huquet D, Walch G, Mole D. Grammont inverted total shoulder arthroplasty in the treatment of glenohumeral osteoarthritis with massive rupture of the cuff. Results of a multicentre study of 80 shoulders. *J Bone Joint Surg Br*. Apr 2004;86(3):388-95. doi:10.1302/0301-620x.86b3.14024
101. Walch G, Collotte P, Raiss P, Athwal GS, Gauci MO. The Characteristics of the Favard E4 Glenoid Morphology in Cuff Tear Arthropathy: A CT Study. *J Clin Med*. Nov 18 2020;9(11)doi:10.3390/jcm9113704

102. O'Neill DC, Christensen GV, Hillyard B, Kawakami J, Tashjian RZ, Chalmers PN. Glenoid retroversion associates with deltoid muscle asymmetry in Walch B-type glenohumeral osteoarthritis. *JSES Int*. Mar 2021;5(2):282-287. doi:10.1016/j.jseint.2020.10.012
103. Hettrich CM, Permeswaran VN, Goetz JE, Anderson DD. Mechanical tradeoffs associated with glenosphere lateralization in reverse shoulder arthroplasty. *J Shoulder Elbow Surg*. Nov 2015;24(11):1774-81. doi:10.1016/j.jse.2015.06.011
104. Jobin CM, Brown GD, Bahu MJ, et al. Reverse total shoulder arthroplasty for cuff tear arthropathy: the clinical effect of deltoid lengthening and center of rotation medialization. *J Shoulder Elbow Surg*. Oct 2012;21(10):1269-77. doi:10.1016/j.jse.2011.08.049
105. Lugli T. Artificial shoulder joint by Pean (1893): the facts of an exceptional intervention and the prosthetic method. *Clin Orthop Relat Res*. Jun 1978;(133):215-8.
106. Neer CS, 2nd. Articular replacement for the humeral head. *J Bone Joint Surg Am*. Apr 1955;37-A(2):215-28.
107. Roberts SN, Foley AP, Swallow HM, Wallace WA, Coughlan DP. The geometry of the humeral head and the design of prostheses. *J Bone Joint Surg Br*. Jul 1991;73(4):647-50. doi:10.1302/0301-620X.73B4.2071652
108. Robertson DD, Yuan J, Bigliani LU, Flatow EL, Yamaguchi K. Three-dimensional analysis of the proximal part of the humerus: relevance to arthroplasty. *J Bone Joint Surg Am*. Nov 2000;82(11):1594-602. doi:10.2106/00004623-200011000-00013
109. Walch G, Boileau P. Prosthetic adaptability: a new concept for shoulder arthroplasty. *J Shoulder Elbow Surg*. Sep-Oct 1999;8(5):443-51. doi:10.1016/s1058-2746(99)90074-5
110. Boileau P, Sinnerton RJ, Chuinard C, Walch G. Arthroplasty of the shoulder. *J Bone Joint Surg Br*. May 2006;88(5):562-75. doi:10.1302/0301-620X.88B5.16466
111. Grammont P TP, Laffay J, Deries X. Concept study and realization of a new total shoulder prosthesis. *Rhumatologie*. 1987;39:407-418.
112. Flatow EL, Harrison AK. A history of reverse total shoulder arthroplasty. *Clin Orthop Relat Res*. Sep 2011;469(9):2432-9. doi:10.1007/s11999-010-1733-6
113. Neer CI. Shoulder Reconstruction. *Philadelphia, PA: WB Saunders*. 1990;
114. Khazzam M FS. History and development of shoulder arthroplasty. *In: Fealy S, Sperling JW, Warren RF, Craig EV, eds Shoulder Arthroplasty New York, NY: Thieme Medical Publishers, Inc*. 2008:1-9.
115. Merolla G. Shoulder replacement in advanced glenohumeral osteoarthritis: current concepts review. *OA Orthopaedics* 2013;1(1):1-15.
116. Merolla G, Paladini P, Campi F, Porcellini G. Efficacy of anatomical prostheses in primary glenohumeral osteoarthritis. *Chir Organi Mov*. Feb 2008;91(2):109-15. doi:10.1007/s12306-007-0019-y
117. Merolla G, Ciaramella G, Fabbri E, Walch G, Paladini P, Porcellini G. Total shoulder replacement using a bone ingrowth central peg polyethylene glenoid component: a prospective clinical and computed tomography study with short- to mid-term follow-up. *Int Orthop*. Nov 2016;40(11):2355-2363. doi:10.1007/s00264-016-3255-7
118. Matsen FA, 3rd, Iannotti JP, Churchill RS, et al. One and two-year clinical outcomes for a polyethylene glenoid with a fluted peg: one thousand two hundred seventy individual patients from eleven centers. *Int Orthop*. Feb 2019;43(2):367-378. doi:10.1007/s00264-018-4213-3
119. Merolla G, Cerciello S, Marenco S, Fabbri E, Paladini P, Porcellini G. Comparison of shoulder replacement to treat osteoarthritis secondary to instability surgery and primary osteoarthritis: a

retrospective controlled study of patient outcomes. *Int Orthop*. Sep 2018;42(9):2147-2157. doi:10.1007/s00264-018-3969-9
120. Merolla G, Chin P, Sasyniuk TM, Paladini P, Porcellini G. Total shoulder arthroplasty with a second-generation tantalum trabecular metal-backed glenoid component: Clinical and radiographic outcomes at a mean follow-up of 38 months. *Bone Joint J*. Jan 2016;98-B(1):75-80. doi:10.1302/0301-620X.98B1.36620
121. Li F, Jiang C. Trabecular metal shoulder prosthesis in the treatment of complex proximal humeral fractures. *Int Orthop*. Nov 2013;37(11):2259-64. doi:10.1007/s00264-013-2061-8
122. Reeves JM, Johnson JA, Athwal GS. An analysis of proximal humerus morphology with special interest in stemless shoulder arthroplasty. *J Shoulder Elbow Surg*. Apr 2018;27(4):650-658. doi:10.1016/j.jse.2017.10.029
123. Campi F DPP, Paladini P, Porcellini G. . Concepts of anatomical, biomechanical, and articular physiology in shoulder arthroplasty. . *In: Porcellini G, Campi F, Paladini P, editors Shoulder replacement in osteoarthritis*. 2005; Bologna, Italy: Timeoeditore:13–34.
124. Grammont P TP, Laffay JP, Deries X. Etude et réalisation d'une nouvelle prothèse d'épaule. *Rhumatologie*. 1987;39:407-418.
125. Matsen FA, 3rd, Boileau P, Walch G, Gerber C, Bicknell RT. The reverse total shoulder arthroplasty. *J Bone Joint Surg Am*. Mar 2007;89(3):660-7. doi:10.2106/00004623-200703000-00027
126. Matsen Iii FA, Boileau P, Walch G, Gerber C, Bicknell RT. The reverse total shoulder arthroplasty. *Instr Course Lect*. 2008;57:167-74.
127. Rugg CM, Coughlan MJ, Lansdown DA. Reverse Total Shoulder Arthroplasty: Biomechanics and Indications. *Curr Rev Musculoskelet Med*. Dec 2019;12(4):542-553. doi:10.1007/s12178-019-09586-y
128. Goetti P, Denard PJ, Collin P, Ibrahim M, Mazzolari A, Ladermann A. Biomechanics of anatomic and reverse shoulder arthroplasty. *EFORT Open Rev*. Oct 2021;6(10):918-931. doi:10.1302/2058-5241.6.210014
129. Levigne C, Garret J, Boileau P, Alami G, Favard L, Walch G. Scapular notching in reverse shoulder arthroplasty: is it important to avoid it and how? *Clin Orthop Relat Res*. Sep 2011;469(9):2512-20. doi:10.1007/s11999-010-1695-8
130. Merolla G. Radiographic features of lateralized reverse shoulder arthroplasty in osteoarthritis. *J Phys Med Rehabil Scientific Archives*. 2022;4(2):49-57.
131. Frankle M, Siegal S, Pupello D, Saleem A, Mighell M, Vasey M. The Reverse Shoulder Prosthesis for glenohumeral arthritis associated with severe rotator cuff deficiency. A minimum two-year follow-up study of sixty patients. *J Bone Joint Surg Am*. Aug 2005;87(8):1697-705. doi:10.2106/JBJS.D.02813
132. Merolla G, Walch G, Ascione F, et al. Grammont humeral design versus onlay curved-stem reverse shoulder arthroplasty: comparison of clinical and radiographic outcomes with minimum 2-year follow-up. *J Shoulder Elbow Surg*. Apr 2018;27(4):701-710. doi:10.1016/j.jse.2017.10.016
133. Smith CD, Guyver P, Bunker TD. Indications for reverse shoulder replacement: a systematic review. *J Bone Joint Surg Br*. May 2012;94(5):577-83. doi:10.1302/0301-620X.94B5.27596
134. Merolla G, Tartarone A, Sperling JW, Paladini P, Fabbri E, Porcellini G. Early clinical and radiological outcomes of reverse shoulder arthroplasty with an eccentric all-polyethylene glenosphere to treat failed hemiarthroplasty and the sequelae of proximal humeral fractures. *Int Orthop*. Jan 2017;41(1):141-148. doi:10.1007/s00264-016-3188-1
135. Merolla G, Wagner E, Sperling JW, Paladini P, Fabbri E, Porcellini G. Revision of failed shoulder hemiarthroplasty to reverse total arthroplasty: analysis of 157 revision implants. *J Shoulder Elbow Surg*. Jan 2018;27(1):75-81. doi:10.1016/j.jse.2017.06.038

136. Chen X, Reddy AS, Kontaxis A, et al. Version Correction via Eccentric Reaming Compromises Remaining Bone Quality in B2 Glenoids: A Computational Study. *Clin Orthop Relat Res*. Dec 2017;475(12):3090-3099. doi:10.1007/s11999-017-5510-7
137. Churchill RS, Spencer EE, Jr., Fehringer EV. Quantification of B2 glenoid morphology in total shoulder arthroplasty. *J Shoulder Elbow Surg*. Aug 2015;24(8):1212-7. doi:10.1016/j.jse.2015.01.007
138. Clavert P, Millett PJ, Warner JJ. Glenoid resurfacing: what are the limits to asymmetric reaming for posterior erosion? *J Shoulder Elbow Surg*. Nov-Dec 2007;16(6):843-8. doi:10.1016/j.jse.2007.03.015
139. Allred JJ, Flores-Hernandez C, Hoenecke HR, Jr., D'Lima DD. Posterior augmented glenoid implants require less bone removal and generate lower stresses: a finite element analysis. *J Shoulder Elbow Surg*. May 2016;25(5):823-30. doi:10.1016/j.jse.2015.10.003
140. Levin JM, Bokshan S, Roche CP, et al. Reverse shoulder arthroplasty with and without baseplate wedge augmentation in the setting of glenoid deformity and rotator cuff deficiency-a multicenter investigation. *J Shoulder Elbow Surg*. Dec 2022;31(12):2488-2496. doi:10.1016/j.jse.2022.04.025
141. Nowak DD, Bahu MJ, Gardner TR, et al. Simulation of surgical glenoid resurfacing using three-dimensional computed tomography of the arthritic glenohumeral joint: the amount of glenoid retroversion that can be corrected. *J Shoulder Elbow Surg*. Sep-Oct 2009;18(5):680-8. doi:10.1016/j.jse.2009.03.019
142. Orvets ND, Chamberlain AM, Patterson BM, et al. Total shoulder arthroplasty in patients with a B2 glenoid addressed with corrective reaming. *J Shoulder Elbow Surg*. Jun 2018;27(6S):S58-S64. doi:10.1016/j.jse.2018.01.003
143. Virk M, Yip M, Liuzza L, et al. Clinical and radiographic outcomes with a posteriorly augmented glenoid for Walch B2, B3, and C glenoids in reverse total shoulder arthroplasty. *J Shoulder Elbow Surg*. May 2020;29(5):e196-e204. doi:10.1016/j.jse.2019.09.031
144. Boileau P, Moineau G, Roussanne Y, O'Shea K. Bony increased-offset reversed shoulder arthroplasty: minimizing scapular impingement while maximizing glenoid fixation. *Clin Orthop Relat Res*. Sep 2011;469(9):2558-67. doi:10.1007/s11999-011-1775-4
145. Ho JC, Thakar O, Chan WW, Nicholson T, Williams GR, Namdari S. Early radiographic failure of reverse total shoulder arthroplasty with structural bone graft for glenoid bone loss. *J Shoulder Elbow Surg*. Mar 2020;29(3):550-560. doi:10.1016/j.jse.2019.07.035
146. Nabergoj M, Neyton L, Bothorel H, et al. Reverse Shoulder Arthroplasty with Bony and Metallic versus Standard Bony Reconstruction for Severe Glenoid Bone Loss. A Retrospective Comparative Cohort Study. *J Clin Med*. Nov 13 2021;10(22)doi:10.3390/jcm10225274
147. Van de Kleut ML, Yuan X, Teeter MG, Athwal GS. Bony increased-offset reverse shoulder arthroplasty vs. metal augments in reverse shoulder arthroplasty: a prospective, randomized clinical trial with 2-year follow-up. *J Shoulder Elbow Surg*. Mar 2022;31(3):591-600. doi:10.1016/j.jse.2021.11.007
148. Abdic S, Knowles NK, Walch G, Johnson JA, Athwal GS. Type E2 glenoid bone loss orientation and management with augmented implants. *J Shoulder Elbow Surg*. Jul 2020;29(7):1460-1469. doi:10.1016/j.jse.2019.11.009
149. Ernstbrunner L, Werthel JD, Wagner E, Hatta T, Sperling JW, Cofield RH. Glenoid bone grafting in primary reverse total shoulder arthroplasty. *J Shoulder Elbow Surg*. Aug 2017;26(8):1441-1447. doi:10.1016/j.jse.2017.01.011

150. Werthel JD, Walch G, Vegehan E, Deransart P, Sanchez-Sotelo J, Valenti P. Lateralization in reverse shoulder arthroplasty: a descriptive analysis of different implants in current practice. *Int Orthop*. Oct 2019;43(10):2349-2360. doi:10.1007/s00264-019-04365-3
151. Favard L, Berhouet J, Walch G, Chaoui J, Levigne C. Superior glenoid inclination and glenoid bone loss : Definition, assessment, biomechanical consequences, and surgical options. *Orthopade*. Dec 2017;46(12):1015-1021. Superiore Glenoidinklination und glenoidaler Knochenverlust : Definition, Assessment, biomechanische Konsequenzen und operative Optionen. doi:10.1007/s00132-017-3496-1
152. Goutallier D, Postel JM, Bernageau J, Lavau L, Voisin MC. Fatty infiltration of disrupted rotator cuff muscles. *Rev Rhum Engl Ed*. Jun 1995;62(6):415-22.
153. Boileau P, Cheval D, Gauci MO, Holzer N, Chaoui J, Walch G. Automated Three-Dimensional Measurement of Glenoid Version and Inclination in Arthritic Shoulders. *J Bone Joint Surg Am*. Jan 3 2018;100(1):57-65. doi:10.2106/JBJS.16.01122
154. Corona K, Cerciello S, Morris BJ, Visona E, Merolla G, Porcellini G. Cross-cultural adaptation and validation of the Italian version of the Western Ontario Osteoarthritis of the Shoulder index (WOOS). *J Orthop Traumatol*. Dec 2016;17(4):309-313. doi:10.1007/s10195-016-0400-4
155. Merolla G. Radiographic Features of Lateralized Reverse Shoulder Arthroplasty in Osteoarthritis. Review. *J Phys Med Rehab* 2022;4(2):49-57.
156. Maurer A, Fucentese SF, Pfirrmann CW, et al. Assessment of glenoid inclination on routine clinical radiographs and computed tomography examinations of the shoulder. *J Shoulder Elbow Surg*. Aug 2012;21(8):1096-103. doi:10.1016/j.jse.2011.07.010
157. Boileau P, Morin-Salvo N, Bessiere C, Chelli M, Gauci MO, Lemmex DB. Bony increased-offset-reverse shoulder arthroplasty: 5 to 10 years' follow-up. *J Shoulder Elbow Surg*. Oct 2020;29(10):2111-2122. doi:10.1016/j.jse.2020.02.008
158. Ho JC, Youderian A, Davidson IU, Bryan J, Iannotti JP. Accuracy and reliability of postoperative radiographic measurements of glenoid anatomy and relationships in patients with total shoulder arthroplasty. *J Shoulder Elbow Surg*. Aug 2013;22(8):1068-77. doi:10.1016/j.jse.2012.11.015
159. Crosby LA, Hamilton A, Twiss T. Scapula fractures after reverse total shoulder arthroplasty: classification and treatment. *Clin Orthop Relat Res*. Sep 2011;469(9):2544-9. doi:10.1007/s11999-011-1881-3
160. Dimock R, Fathi Elabd M, Imam M, Middleton M, Godeneche A, Narvani AA. Bony increased-offset reverse shoulder arthroplasty: A meta-analysis of the available evidence. *Shoulder Elbow*. Feb 2021;13(1):18-27. doi:10.1177/1758573220916848
161. Colasanti CA, Lin CC, Ross K, et al. Augmented Baseplates Yield Optimum Outcomes When Compared to Bone Graft Augmentation for Managing Glenoid Deformity During Reverse Total Shoulder Arthroplasty-A Retrospective Comparative Study. *J Shoulder Elbow Surg*. Nov 15 2022;doi:10.1016/j.jse.2022.10.015
162. Kirsch JM, Patel M, Singh A, Lazarus MD, Williams GR, Namdari S. Early clinical and radiographic outcomes of an augmented baseplate in reverse shoulder arthroplasty for glenohumeral arthritis with glenoid deformity. *J Shoulder Elbow Surg*. Jul 2021;30(7S):S123-S130. doi:10.1016/j.jse.2020.12.010
163. Ricchetti ET, Hendel MD, Collins DN, Iannotti JP. Is premorbid glenoid anatomy altered in patients with glenohumeral osteoarthritis? *Clin Orthop Relat Res*. Sep 2013;471(9):2932-9. doi:10.1007/s11999-013-3069-5

164. Zhou Y ER, Van Niekerk M, Hirner M. Reverse shoulder arthroplasty with metallic augments to preserve bone and restore joint line in patients with glenoid bone loss. *Seminars in Arthroplasty*. 2022;(Epub June, 10 2022):1-10. doi:10.1053/j.sart.2022.05.001
165. Ferreira LM, Knowles NK, Richmond DN, Athwal GS. Effectiveness of CT for the detection of glenoid bone graft resorption following reverse shoulder arthroplasty. *Orthop Traumatol Surg Res*. Jun 2015;101(4):427-30. doi:10.1016/j.otsr.2015.03.010
166. Franceschetti E, Ranieri R, Giovanetti de Sanctis E, Palumbo A, Franceschi F. Clinical results of bony increased-offset reverse shoulder arthroplasty (BIO-RSA) associated with an onlay 145 degrees curved stem in patients with cuff tear arthropathy: a comparative study. *J Shoulder Elbow Surg*. Jan 2020;29(1):58-67. doi:10.1016/j.jse.2019.05.023
167. Tashjian RZ, Granger E, Chalmers PN. Structural glenoid grafting during primary reverse total shoulder arthroplasty using humeral head autograft. *J Shoulder Elbow Surg*. Jan 2018;27(1):e1-e8. doi:10.1016/j.jse.2017.07.010